HHS Public Access

Author manuscript

Hear Res. Author manuscript; available in PMC 2023 March 06.

Published in final edited form as:

Hear Res. 2022 December ; 426: 108643. doi:10.1016/j.heares.2022.108643.

Comparison of response properties of the electrically stimulated auditory nerve reported in human listeners and in animal models

Jeffrey Skidmore, PhD[1], **Dyan Ramekers, PhD**[2,3], **Ian C. Bruce, PhD**[4], **Shuman He, MD, PhD**[1,5]

[1]Department of Otolaryngology – Head and Neck Surgery, The Ohio State University, 915 Olentangy River Road, Columbus, OH 43212, USA

[2]Department of Otorhinolaryngology and Head & Neck Surgery, University Medical Center Utrecht, Utrecht University, Room G.02.531, P.O. Box 85500, 3508 GA Utrecht, The Netherlands

[3]UMC Utrecht Brain Center, Utrecht University, Utrecht, The Netherlands

[4]Department of Electrical & Computer Engineering, McMaster University, 1280 Main Street West, Hamilton, ON, L8S 4K1, Canada

[5]Department of Audiology, Nationwide Children's Hospital, 700 Children's Drive, Columbus, OH 43205, USA

Abstract

Cochlear implants (CIs) provide acoustic information to implanted patients by electrically stimulating nearby auditory nerve fibers (ANFs) which then transmit the information to higher-level neural structures for further processing and interpretation. Computational models that simulate ANF responses to CI stimuli enable the exploration of the mechanisms underlying CI performance beyond the capacity of *in vivo* experimentation alone. However, all ANF models developed to date utilize to some extent anatomical/morphometric data, biophysical properties and/or physiological data measured in non-human animal models. This review compares response properties of the electrically stimulated auditory nerve (AN) in human listeners and different mammalian models. Properties of AN responses to single pulse stimulation, paired-pulse stimulation, and pulse-train stimulation are presented. While some AN response properties are similar between human listeners and animal models (e.g., increased AN sensitivity to single pulse stimuli with long interphase gaps), there are some significant differences. For example, the AN of most animal models is typically more sensitive to cathodic stimulation while the AN of human listeners is generally more sensitive to anodic stimulation. Additionally, there are substantial differences in the speed of recovery from neural adaptation between animal models and human listeners. Therefore, results from animal models cannot be simply translated to human listeners. Recognizing the differences in responses of the AN to electrical stimulation between humans and

Correspondence: Shuman He, MD, PhD, Eye and Ear Institute, Department of Otolaryngology – Head and Neck Surgery, The Ohio State University, 915 Olentangy River Road, Suite 4000, Phone: 614-293-5963, Fax: 614-293-7292, Shuman.He@osumc.edu.
Author Contributions: Jeffrey Skidmore: Writing-Original draft preparation, reviewing and editing. Dyan Ramekers: Writing-Original draft preparation, reviewing and editing. Ian C. Bruce: Writing-Original draft preparation, reviewing and editing. Shuman He: Conceptualization, funding acquisition, investigation, writing- Original draft preparation, reviewing and editing.

Declarations of Interest: None.

other mammals is an important step for creating ANF models that are more applicable to various human CI patient populations.

Keywords

electrical stimulation; animal models; human cochlear implant users; auditory nerve; response characteristics; electrically evoked auditory compound action potentials

INTRODUCTION

The cochlear implant (CI) is one of the most successful implantable medical devices in history. CIs convey acoustic information to implanted patients by electrically stimulating auditory nerve fibers (ANFs) within the cochlea. While most adult patients have improvement in speech perception after receiving a CI (e.g., Bittencourt et al., 2012; Hey et al., 2020; Rasmussen et al., 2022), 10 to 50% are still considered as “poor performers” (Lenarz et al., 2012; Rumeau et al., 2015; Moberly et al., 2016). There is also a wide range of speech perception skills among pediatric CI users. Performance ranges from no awareness of environmental sounds to conversation without lipreading (Galvin et al., 2007; Birman et al., 2016; Han et al., 2019). A comprehensive understanding of how electrical stimulation is encoded and processed in the auditory nerve (AN) may help explain a portion of the variability in CI outcomes and provide insight for improving speech perception for CI patients.

Computational modeling techniques are extremely valuable tools for providing insightful information about how electrical stimulation is encoded and processed in healthy and impaired ANFs. Overall, these computational models can be classified into two categories: biophysical and phenomenological. Biophysical models simulate the biophysical mechanisms of ANFs by incorporating detailed mathematical formulations that represent the corresponding physiological functions of actual ANFs. In contrast, phenomenological models simulate observable aspects of ANFs (e.g., firing threshold, response latency, refractory properties) using simplified mathematical formulations that may not have a direct biophysical interpretation. Despite the fundamental difference in these two types of ANF models, almost all ANF models developed to date utilize some amount of anatomical/morphometric data, biophysical properties and/or physiological data measured in non-human animal models, such as cat (Colombo & Parkins, 1987; Bruce et al., 1999a, b, c; Goldwyn et al., 2012; Rattay et al., 2013; Horne et al., 2016; Joshi et al., 2017), guinea pig (Frijns et al., 1995), squirrel monkey (Parkins & Colombo, 1987), or squid (Motz & Rattay, 1986; Rattay, 1990). Many ANF models utilize data from more than one animal species (e.g., Imennov & Rubinstein, 2009; Woo et al., 2009a, b, 2010; Miller et al., 2011; Negm & Bruce, 2014; Boulet & Bruce, 2017). The authors of these modeling studies did not provide a rationale for the choice of animal. Presumably, the key factor was the availability of the physiologic results.

There are some crucial issues that need to be considered when developing computational models of ANFs for human CI users. First, there are substantial differences in anatomical/morphometric and biophysical properties of ANFs between human listeners and other

mammalian species (e.g., Ota & Kimura, 1980; Liberman & Oliver, 1984; Nadol, 1988; Felix et al., 1992; Liu et al., 2012; Rattay et al., 2013; Kroon et al., 2017; Ramekers et al., 2020). For example, for Type I spiral ganglion neurons (SGNs) the area of the SGN body, the diameters of the peripheral and central axons, the number of internodal compartments preceding the SGN body, and the internodal length vary substantially across mammalian species (Liberman & Oliver, 1984; Nadol, 1988; Felix et al., 1992; Rattay et al., 2001a; Rattay et al., 2013; Kroon et al., 2017; Ramekers et al., 2020), which affects the conduction velocities of action potentials. More importantly, in contrast to other mammalian species, cell bodies of all standard Type II and the majority of Type I SGNs, as well as their pre- and post-somatic segments, are not tightly myelinated in humans (Ota & Kimura, 1980; Nadol, 1988; Liu et al., 2012; Rattay et al., 2013), which could result in remarkable differences in spike generation and spike conduction between humans and other mammalian species (Rattay et al., 2001a; Rattay et al., 2013). Second, the volume of the cochlea is larger in humans than many nonhuman animals (e.g., Kirk & Gosselin-Ildari, 2009; Trinh et al., 2021) which affects compound AN response amplitudes and excitation patterns due to resulting differences in the electrode-neuron distance and the spread of electrical current within the cochlea (Kopsch et al., 2022). Third, aging and/or long-duration of deafness can cause AN degeneration in human CI users (e.g., Makary et al., 2011; Viana et al., 2015; Wu et al., 2019), which leads to the difference in the health status of the AN between human CI users and animal models with healthy ANs, or with acute or relatively short-term deafness. Finally, in contrast to the controlled and acute deafening of animal models, the etiology of hearing loss among CI users is highly variable and impacts various aspects of the auditory pathway (e.g., Miyagawa et al., 2016; Shearer et al., 2017).

Due to these fundamental differences, ANF models based on results measured in animal models may not be fully applicable to human CI users. Liu et al. (2020) tried to address this critical issue by attempting to build a patient-specific model. However, this model was created with the “warmed” Hodgkin-Huxley model (Motz & Rattay, 1986; Rattay, 1990) which includes ion channel dynamics based on the unmyelinated squid membrane. Smit et al. (2008, 2009, 2010) incorporated ion channel dynamics measured in humans into their ANF model. However, the ion channel data were recorded in non-auditory peripheral nerve fibers (e.g., sciatic, ulnar, sural, medial cutaneous), and the model failed to accurately predict behavioral detection thresholds (i.e., the validation data) at various pulse rates (Smit et al., 2010). Recently, Bachmaier et al. (2019) implemented three of the most cited biophysical ANF models and found that none of the models satisfactorily predicted AN response properties from experimental data. To date, there is still no ANF model that is validated exclusively based on results measured in human listeners.

There is increasing evidence of some differences in neural response properties of the AN to electrical stimulation between human listeners and different mammalian models. Recognizing these differences is important for creating valid ANF model(s) that can be applicable to various CI patient populations. This review describes response properties of the electrically stimulated AN to single-pulse stimulation, paired-pulse stimulation, and pulse-train stimulation reported in human CI users as well as in various animal models. The relationship between AN response properties and the neural status of the AN (i.e., survival and health of SGNs) is also discussed. In this review, neural survival refers to the number

of surviving SGN cell bodies, while neural health refers to the condition of the SGNs (e.g., size, degeneration of peripheral processes, demyelination). This differentiation is especially important when considering aging effects because many SGNs survive with only central axons intact in the aging cochlea (e.g., Wu et al., 2019).

In animal models, neural response properties of the electrically stimulated AN can be assessed using single-fiber recording. These response properties include firing rate, firing efficiency (firing probability), response latency, response jitter, vector strength, Fano factor (an index of the temporal variability of responsiveness), strength-duration curve, etc. In both human CI users and animal models, AN response properties can also be evaluated using various testing paradigms for measuring the electrically evoked compound action potential (eCAP). The eCAP is a near-field recorded neural response generated by multiple ANFs. Its presence depends on the existence of sufficient ANFs responding synchronously to electrical stimulation. The eCAP recorded using an intra-cochlear CI electrode typically consists of a negative peak (N1) followed by a positive peak (P2). Peak latencies are affected by the overall functional status (the number and responsiveness of surviving neural elements) of the AN in both animal models (Ramekers et al., 2014, 2015a) and human CI users (Skidmore & He, 2021). Due to the infeasibility of conducting single-fiber recording in human CI users, this review focuses on the difference in eCAP results between human listeners and animal models. It should be pointed out that observed differences in eCAP measures could have contributing factors at both the cellular level and the population level. For example, a longer refractory recovery time constant measured using an eCAP testing paradigm might reflect longer recovery from refractoriness for each of the individual SGNs, increased jitter across the population of SGNs, or a combination of the two mechanisms. In contrast, studies using single-fiber recordings can directly measure the refractory properties of individual SGNs. Therefore, results of single-fiber recordings in animal models that are informative for understanding and explaining eCAP data are also reported.

2. RESPONSE PROPERTIES

2.1. Response Properties to Single-Pulse Stimulation

In this review, neural response evoked by single-pulse stimulation refers to the response elicited by a single electrical pulse with either one phase or multiple phases. The eCAP evoked using the classic two-pulses forward masking technique (Brown et al., 1990) where one electrical pulse serves as the masker and the other pulse serves as the probe is still considered as a neural response evoked by single-pulse stimulation because the first pulse (i.e., masker) is used to remove the stimulation artifact. Testing paradigms using single pulse stimulation can be used to evaluate the inherent responsiveness of the electrode-neuron interface and the sensitivity of responsiveness to changes in stimulation parameters of a single pulse.

The characteristics of a single pulse (i.e., the pulse shape) are defined by the number of pulse phases along with the shape, amplitude (i.e., current level), polarity and duration of each phase. In the case of a single pulse with multiple phases, a zero-amplitude period may be inserted between the nonzero amplitude phases (i.e., interphase gap [IPG]). The defining characteristics of a single pulse are illustrated in Figure 1A. Single pulses with

constant pulse amplitude through the pulse phase (i.e., rectangular pulses) are used clinically in CIs and have been used in all research studies that recorded eCAPs in animal models and CI users. Ramped pulses have recently been utilized in an electrically evoked auditory brainstem response (eABR) study with mice (Navntoft et al., 2020) and a perceptual study with CI users (Navntoft et al., 2021). This review only includes results from studies implementing rectangular pulses due to its clinical relevance and the lack of eCAP studies implementing non-rectangular pulse stimuli. Illustrations of various rectangular pulse shapes used in studies referenced in this review are provided in Figure 1B.

The shape of the single pulse affects the responsiveness of the AN to the electrical stimulation. In this section, the sensitivity of the AN to changes in pulse amplitude, pulse polarity, pulse phase duration (PPD), IPG, and number of pulse phases are compared between animal models and human CI users.

2.1.1. Sensitivity to Pulse Amplitude—The eCAP amplitude increases monotonically with pulse amplitude (i.e., current level) in most cases. This increase is due to better firing synchrony, higher firing rates and the recruitment of more fibers at higher stimulation levels (van den Honert & Stypulkowski, 1984). The eCAP amplitude growth function (AGF) represents changes in the eCAP amplitude as stimulation level increases. The three most common parameters extracted from the eCAP AGF are the lowest stimulation level that evokes an eCAP (i.e., the eCAP threshold), the maximum eCAP amplitude, and the rate at which the eCAP amplitude increases with stimulation level (i.e., the slope of the eCAP AGF).

2.1.1.1. Studies in animal models: The ranges of reported eCAP thresholds, maximum eCAP amplitudes, and slopes of the eCAP AGF vary across animal species (Miller et al., 1998), and depend on the number of ANFs (Ramekers et al., 2014; Pfingst et al., 2015a, b; Pfingst et al., 2017; Schvartz-Leyzac et al., 2019, Vink et al., 2020), the electrode-neuron interface (Ramekers et al., 2015b; Schvartz-Leyzac et al., 2019; Ramekers et al., 2022), and the pulse shape (Miller et al., 1998; Ramekers et al., 2014; Schvartz-Leyzac et al., 2019).

In guinea pigs, the eCAP threshold and the slope of the eCAP AGF range from approximately 2.6 to 24.0 nanocoulombs (nC) and from approximately 14 to 1700 μV/nC, respectively. The largest eCAP amplitudes reported in guinea pigs range from approximately 1800 to 3100 μV. Importantly, both the maximum eCAP amplitude and the slope of the eCAP AGF have repeatedly been shown to be associated with SGN density, with larger maximum eCAP amplitudes and steeper slopes indicating greater SGN density (Ramekers et al., 2014; Pfingst et al., 2015a, b; Pfingst et al., 2017; Schvartz-Leyzac et al., 2019, Vink et al., 2020). These results are consistent with an eABR study that reported larger amplitudes of the first positive peak (i.e., wave I) and steeper wave I growth functions in rats with greater SGN survival (Hall, 1990). The maximum eCAP amplitude and the slope of the eCAP AGF explain approximately 49 – 71% and 48 - 67% of the variance in SGN density, respectively (Ramekers et al., 2014; Vink et al., 2020). The latency of the first negative peak in the eCAP waveform (i.e., N1 latency) recorded with an intracochlear electrode at the highest stimulation level has also been shown to correlate with neural survival, where shorter N1 latencies reflect smaller SGN size, lower SGN density and longer duration of

deafness (Ramekers et al., 2014, 2015a). These results align with the theory that shorter response latencies would be expected for smaller SGN size and lower SGN density due to faster depolarization of smaller cells and a more direct path of stimulation current to sparsely packed cells. Additionally, Ramekers et al. (2014) suggested that differences in the sensitivity to the cathodic-leading and anodic-leading pulses between healthy and impaired ANFs might have also contributed to the observed association between N1 latency and neural survival. Schvartz-Leyzac et al. (2019) reported no significant group difference in N1 latency measured using an intracochlear electrode between deafened and non-deafened guinea pigs despite group differences in SGN density. The apparent discrepancy between Ramekers et al. (2014, 2015a) and Schvartz-Leyzac et al. (2019) is not well understood but may be influenced by differences in the PPD of the stimuli, the duration of deafness of the animals and the stimulation levels at which N1 latency was recorded. These three factors have been shown to affect N1 latency (Miller et al., 2003; Ramekers et al., 2014, 2022). The eCAP threshold has not been shown to be correlated with SGN density (Ramekers et al., 2014; Vink et al., 2020).

Inconsistencies in some, but not all, eCAP results recorded in different animal models have also been reported. For example, Miller et al. (1998) reported that eCAP thresholds measured in cats (range: 6.9 - 42.2 nC) were significantly higher than eCAP thresholds measured in guinea pigs (range: 2.6 – 24.0 nC) at all pulse durations evaluated. The authors noted that significant anatomical differences of the cochlea between cats and guinea pigs could contribute to between-species differences in recorded neural responses (Miller et al., 1998). However, there was no significant difference in the maximum eCAP amplitude between these two animal models (Miller et al., 1998).

2.1.1.2. Studies in human CI users: The ranges of eCAP thresholds, maximum eCAP amplitudes, and slopes of the eCAP AGF reported in human CI listeners vary across patient populations (He et al., 2018, 2020a, b; Luo et al., 2020; Xu et al., 2020; Skidmore et al., 2021, 2022a, b), the region of the cochlea tested (He et al., 2018, 2020a, b; Hughes et al., 2018; Luo et al., 2020; Skidmore et al., 2021), the pulse shape (Hughes et al., 2018; He et al., 2020a, b; Xu et al., 2020), and the CI manufacturer (Hughes et al., 2017, 2018; Hughes, 2022). In general, lower eCAP thresholds, larger eCAP amplitude, and steeper slopes of the eCAP AGF are reported in patient populations with better AN survival and/or health (He et al., 2018, 2020b; Luo et al., 2020; Xu et al., 2020), as established by histological results of human temporal bones (Jun et al., 2000; Nelson & Hinojosa, 2001; Chen et al., 2019; de Costa Monsanto et al., 2022). These temporal bone studies showed that individuals with cochlear nerve deficiency (CND) have substantially fewer spiral ganglion neurons (i.e., poor neural survival) than age-matched controls (Nelson & Hinojosa, 2001; Chen et al., 2019; de Costa Monsanto et al., 2022). In comparison, Jun et al. (2000) reported good preservation of SGNs and no neural degeneration in hearing loss caused by Gap Junction Beta-2 genetic mutations. For adult CI users, lower eCAP thresholds and steeper slopes have been reported in the apex than in the base of the cochlea (Cafarelli Dees et al., 2005; Brill et al., 2009; Brown et al., 2010; Hughes et al., 2018; Skidmore et al., 2021, 2202a), which agrees with the observation that adult listeners with sensorineural hearing loss (SNHL) tend to have better AN survival and health in the apical region than in the basal region of the cochlea

(Zimmermann et al., 1995). However, a shorter electrode-to-neuron distance caused by a smaller cross-sectional area in the apical region of the cochlea likely also contributes to lower eCAP thresholds and steeper AGF slopes in the apex for adult CI users. In contrast, pediatric CI users with small or absent ANs (i.e., children with CND) have lower eCAP thresholds and steeper slopes in the base of the cochlea compared to the apex (He et al., 2018, 2020b; Luo et al., 2020; Xu et al., 2020). This result agrees with the expected pattern of neural survival in children with CND resulting from arrested base-to-apex development of the AN during embryogenesis (Jackler et al., 1987; He et al., 2018). For all CI patient populations, lower eCAP thresholds and larger eCAP amplitudes are observed with stimuli with longer IPGs (Schvartz-Leyzac & Pfingst, 2016, 2018; Hughes et al. 2018; He et al., 2020b; Imsiecke et al., 2021; Langner et al., 2021) and stimuli with fewer pulse phases (Bahmer & Baumann, 2013; Herrmann et al., 2021). Recently, Hughes (2022) reported larger eCAP amplitudes in CI users with Advanced Bionics devices than for CI users with devices from Cochlear Americas for very similar stimuli, although it is not clear whether this is due to the difference in device or patient population.

In human CI users, the eCAP threshold and the eCAP amplitude at the maximum comfort level range from approximately 2.2 to 20.0 nC and from approximately 25 to 1200 μV, respectively. Ranges for the slope of the eCAP AGF are less meaningful in human CI users due to the wide variety of methods and/or unit scales used to quantify the slope (Skidmore et al., 2022b). Despite differences in quantifying the slope of the eCAP AGF, results from various studies with human CI users showed that steeper slopes were associated with better AN survival and/or health. Specifically, an age-related decline in the slope of the eCAP AGF has been reported consistently in the literature (Cafarelli Dees et al., 2005; Jahn & Arenberg, 2020a, b; Mussoi & Brown, 2020; Shader et al., 2020; Skidmore et al., 2022a). In addition, children with CND have shallower eCAP AGF slopes than age-matched children with normal-sized ANs (He et al., 2018, 2020b). Children with CND have also been shown to have longer N1 latencies than children with normal-sized ANs when recorded with an intracochlear electrode at the maximum comfort level (Xu et al., 2020). This result suggests that longer N1 latencies indicate poorer SGN survival in human CI users.

2.1.1.3. Summary: Three relationships are observed when comparing eCAP parameters extracted from the eCAP AGF between animal models and human CI users. First, larger eCAP amplitudes can be obtained in animal models than in human CI users. This may be due, at least in part, to smaller electrode-neuron distances because of smaller cochlea in animal models and the inability to reach the eCAP saturation plateau in many human CI users because of device limitations or subject discomfort. Secondly, there is strong evidence to suggest that the slope of the eCAP AGF reflects the underlying neural condition in animals and humans. Specifically, the eCAP amplitude increases faster with increasing stimulation level (i.e., steeper slope) in animals and humans with better neural health and better neural survival because of increased firing synchrony, higher firing rates and the recruitment of more ANFs at higher stimulation levels (van den Honert & Stypulkowski, 1984). Finally, there appears to be a different relationship regarding neural survival and the N1 latency between animal models and human CI users. Specifically, poorer neural survival is usually associated with *shorter* N1 latencies in animal models, while poorer

neural survival is associated with *longer* N1 latencies in pediatric CI users. However, only a limited number of studies have reported the relationship between neural survival and N1 latency which precludes a definitive conclusion.

2.1.2. Sensitivity to Stimulus Polarity—Both cathodic and anodic stimuli can initiate action potentials in extracellular AN stimulation (van den Honert & Stypulkowski, 1984; Miller et al., 1998, 2004; Shepherd & Javel, 1999; van Wieringen et al., 2008; Undurraga et al., 2013). Results from computational models and animal studies suggest that cathodic stimulation initiates action potentials more peripherally, while anodic stimulation initiates action potentials more centrally (Parkins, 1989; Rattay et al., 2001a, b; Rubinstein et al., 2001; Miller et al., 2004, Joshi et al., 2017). The possible site of excitation, and therefore the sensitivity of the AN to stimulus polarity, can be influenced by the number of ANFs, the degree of degeneration of the peripheral process, and the extent of demyelination of ANFs (Rattay, 1999; Rattay et al., 2001a, b; Resnick et al., 2018).

2.1.2.1. Studies in animal models: Results from animal models generally indicate that the AN is more sensitive to cathodic stimulation (Hartmann et al., 1984; Miller et al., 1998, 1999a, 2004; Klop et al., 2004; Macherey & Cazals, 2016). For example, eCAP thresholds were lower and slopes of the eCAP AGF were greater for monophasic cathodic stimuli than for monophasic anodic stimuli in cats (Miller et al., 1998, 1999a, 2004). Similarly, the cathodic phase of sinusoidal stimuli was shown to be more effective than the anodic phase in single-fiber recordings from cats (Hartmann et al., 1984). In guinea pigs, Klop et al. (2004) reported shorter N1 latencies in eCAPs recorded at the round window for cathodic-first biphasic stimuli than for anodic-first biphasic stimuli at all current levels tested, which could be due to greater AN sensitivity to cathodic stimulation. Similarly, larger amplitudes of the inferior colliculus evoked potential were recorded in guinea pigs for cathodic pseudo-monophasic stimuli, cathodic-leading biphasic stimuli, and cathodic-dominant triphasic stimuli compared to the analogous anodic stimuli (Macherey & Cazals, 2016). However, a couple of studies have reported either no differences between polarities or greater sensitivity to anodic stimulation in animal models (Miller et al., 1998; Konerding et al., 2022). Specifically, Miller et al. (1998) reported that guinea pigs had lower monophasic anodic eCAP thresholds than cathodic monophasic eCAP thresholds, which was the opposite of the result that they reported for cats in the same study. The apparent discrepancy between species in the Miller et al. (1998) study remains unknown, but may include differences in electrode geometry, neural properties, neural survival, and anatomy of the cochlea (Miller et al., 1999b). Additionally, Konerding et al. (2022) recently reported shorter eCAP latencies for anodic-leading compared to cathodic-leading biphasic stimuli recorded at the round window, which is the opposite result presented in Klop et al. (2004). The reasons for the apparent opposite result between Klop et al. (2004) and Konerding et al. (2022) remain unknown but may be influenced by the peak used in the analysis (N1 vs N2). Konerding et al. (2022) also reported no differences in eCAP threshold, maximum eCAP amplitude, or slope of the eCAP AGF between the stimuli of opposite polarity.

2.1.2.2. Studies in human CI users: In general, results of studies with CI users show higher AN sensitivity to anodic-leading biphasic and anodic-dominant triphasic stimuli

compared to the cathodic equivalent stimuli at suprathreshold levels (Macherey et al., 2008; Undurraga et al., 2010; Bahmer & Baumann, 2013; Spitzer & Hughes, 2017; Hughes et al., 2017, 2018; Luo et al., 2020; Xu et al., 2020; Herrmann et al., 2021; Hughes, 2022). Specifically, most studies have reported that anodic stimulation (i.e., anodic-leading or anodic-dominant), compared to cathodic stimulation, results in larger eCAP amplitudes at fixed stimulation levels (Macherey et al., 2008; Undurraga et al., 2010; Bahmer & Baumann, 2013; Spitzer & Hughes, 2017; Hughes et al., 2017, 2018; Luo et al., 2020; Xu et al., 2020; Herrmann et al., 2021; Hughes, 2022), steeper slopes of the eCAP AGF (Hughes et al., 2017, 2018; Luo et al., 2020; Xu et al., 2020; Hughes, 2022), broader spread of excitation (Spitzer & Hughes, 2017), and shorter N1 latencies measured with intracochlear electrodes (Macherey et al., 2008; Undurraga et al., 2010; Hughes et al., 2017, 2018; Xu et al., 2020; Hughes, 2022). Interestingly, Hughes and colleagues reported that anodic-leading biphasic pulses resulted in larger eCAP amplitudes and steeper eCAP AGFs than cathodic-leading pulses in patients with Cochlear Americas devices but not in patients with Advanced Bionics devices, even when using the same artifact reduction technique for both manufacturers (Hughes et al., 2017, 2018). Hughes (2022) systematically compared the eCAP responses obtained with the forward masking artifact reduction technique between manufacturers at very similar IPGs and PPDs and found the same results as the earlier studies. Therefore, the apparent difference in eCAP sensitivity to stimulus polarity between CI manufacturers reported in Hughes (2022) remains unknown. However, approximately half (7/15) of the patients with Advanced Bionics devices were children while only one of the 16 patients with Cochlear Americas devices was a child. This difference in patient demographics (e.g., age and etiology of hearing loss) could have influenced the study results. Additionally, Hughes (2022) identified inherent differences between manufacturers that might account for the observed differences in polarity sensitivity. These differences include noise floor (Cochlear Americas: 2 – 4 μV; Advanced Bionics: 20 – 40 μV), amplifier linearity, probe repetition rate, and the design of the electrode array. However, Macherey et al. (2008) and Undurraga et al. (2010) reported significant differences in sensitivity to pulse polarity for patients with Advanced Bionics devices using the forward masking artifact reduction technique. These apparent discrepancies in results for the same CI manufacturer remain unclear but may be influenced by differences in patient demographics (age and etiology of hearing loss) and relatively small sample sizes.

Studies investigating the polarity effect on the eCAP threshold have shown mixed results. Specifically, some studies reported lower eCAP thresholds for anodic-leading biphasic pulses than for cathodic-leading biphasic pulses in pediatric patient populations (Luo et al., 2020; Xu et al., 2020). This significant difference was not observed in other studies (Karg et al., 2013; Hughes et al., 2017, 2018; Hughes, 2022). The reason for this apparent discrepancy in results at the group level remains unknown but is likely impacted by the demographics of the patients enrolled in each study. Specifically, the studies indicating significant differences in eCAP threshold only tested pediatric CI users with various etiologies of hearing loss (Luo et al., 2020; Xu et al., 2020) while the participants in the studies reporting no polarity differences were exclusively adult CI users (Karg et al., 2013) or mostly adult CI users with a few pediatric CI users (Hughes et al., 2017, 2018; Hughes, 2022). At the individual level, the direction of the polarity effect on the eCAP threshold

(i.e., higher cathodic threshold vs higher anodic threshold) varies across subjects and across electrode locations within the same subject (Karg et al., 2013; Hughes et al., 2018; Luo et al., 2020; Xu et al., 2020). Therefore, it is highly likely that AN sensitivity to the polarity of the stimulus is influenced by the local neural condition (i.e., survival/health) at individual electrode locations.

2.1.2.3. Summary: The consensus of the available literature indicates generally opposite AN sensitivity to pulse polarity between most animal models and human CI users. Specifically, the AN of most animal models is more sensitive to cathodic stimulation while the AN of human CI users is typically more sensitive to anodic stimulation. Figure 2 shows the means and standard deviations of eCAP amplitudes and N1 latencies obtained in four patient populations for cathodic-leading and anodic-leading biphasic stimulation. Part of these data have been reported in two recent studies (Luo et al., 2020; Xu et al., 2020). Results from one-tailed, paired-sample t-tests indicated significant polarity differences in the eCAP amplitude and the N1 latency for each of the four patient populations ($p<0.001$ for all tests).

2.1.3. Sensitivity to Changes in the Pulse Phase Duration—The amount of charge delivered during a stimulation phase is equal to the pulse amplitude (i.e., current) integrated over the phase duration (i.e., time). Therefore, increasing the PPD with a constant amplitude proportionally increases the amount of charge delivered to the AN. However, prolonged PPDs do not necessarily guarantee improved neural responsiveness to electrical stimulation due to the 'leakiness' of the neural membrane (Lapicque, 1907; Abbas & Brown, 1991; Parkins & Colombo, 1987; Shepherd & Javel, 1999; van den Honert & Stypulkowski, 1984).

The relationship between neural responsiveness and PPD is characterized by the strength–duration function, which is obtained by plotting physiologic thresholds as a function of PPD (Loeb et al., 1983; van den Honert & Stypulkowski, 1984; Parkins & Colombo, 1987; Abbas & Brown, 1991; Shepherd et al., 2001). As demonstrated by the strength-duration function presented in Figure 3A, less *current* is required to evoke a neural response when using stimuli with longer PPDs. However, the total minimal *charge* required to evoke the neural response is larger at longer PPDs, as shown in Figure 3B. Based on the data presented in Figure 3B, approximately 14% more charge is needed to evoke an eCAP with a PPD of 88 μs than is needed with a PPD of 25 μs. In summary, for the PPDs shown in Figure 3, stimuli with shorter PPDs are more effective at stimulating the AN (i.e., require less charge) than stimuli with longer PPDs due to the 'leakiness' of the neural membrane.

Additionally, the change in AN responsiveness resulting from a change in the PPD (i.e., PPD effect) may reflect the underlying neural condition of the AN. Specifically, neural demyelination results in reduced membrane resistance allowing more charge to 'leak' across the membrane (Koles & Rasminsky, 1972; Spoendlin, 1984), which leads to increased PPD effects.

2.1.3.1. Studies in animal models: Results of animal studies have repeatedly shown that firing thresholds decrease with increased PPD when maintaining the pulse amplitude

and thus increasing the total charge delivered. This has been shown for eCAP thresholds measured in guinea pigs (Miller et al., 1998; Prado-Guitierrez et al., 2006) and cats (Miller et al., 1998), eABR thresholds measured in guinea pigs (Miller et al., 1995; Prado-Guitierrez et al., 2006), and single-fiber thresholds recorded in squirrel monkeys (Parkins & Colombo, 1987) and cats (van den Honert & Stypulkowski, 1984; Shepherd & Javel, 1999; Shepherd et al., 2001). At equal charge levels, the effect of increasing the PPD on the eCAP threshold is influenced by the IPG of the biphasic pulse. Specifically, Ramekers et al. (2014) reported decreasing thresholds with increasing PPD (range: 20 – 50 μs) when the IPG was 2.1 μs, but no difference in thresholds at different PPDs (range: 20 – 50 μs) when the IPG was 30 μs in acutely implanted guinea pigs. For a biphasic stimulus with an IPG of 15 μs, Adenis et al. (2018) reported a significant decrease in eCAP threshold when the PPD was increased from 21 μs to 30 μs in chronically implanted guinea pigs. These combined results suggest that neural responsiveness is increased with increasing PPD (for PPDs between 20 and 50 μs) for shorter IPGs (i.e., <15 μs) but not at longer IPGs (i.e., ≥30 μs). Ramekers et al. (2014) proposed that this phenomenon may indicate that PPD and IPG both affect neural responsiveness by the same mechanism of increasing the time between the leading and lagging phases of a biphasic pulse, thereby reducing the likelihood of an action potential generated by the leading phase being abolished by the lagging phase (van den Honert & Mortimer, 1979; Shepherd & Javel, 1999). According to this principle, reduced thresholds would be expected with increased PPDs due to the increased temporal separation between the leading and lagging phases, at least for biphasic pulses with short PPDs (i.e., ≤ 50 μs) and short IPGs (i.e., <15 μs). However, the influence of increasing the PPD would be expected to be negligible for biphasic pulses with long IPGs because of the existing separation between the phases. Consistent with these expectations, Ramekers et al. (2014) also reported larger eCAP amplitudes and steeper slopes of the eCAP AGF at longer PPDs with an IPG of 2.1 μs but not with an IPG of 30 μs and Miller et al. (1998) presented similar eCAP amplitudes with different PPDs (range: 26 – 76 μs) in both guinea pigs and cats when using an IPG of 30 μs.

The magnitude of the effect of PPD on physiologic threshold has also been shown to reflect the underlying neural condition in guinea pigs (Prado-Guitierrez et al., 2006; Ramekers et al., 2014). Prado-Guitierrez et al. (2006) reported that the difference in current required to evoke eABRs of equal amplitude when the PPD was increased from 104 to 208 μs was positively correlated with SGN density. This indicated that the animals with better neural survival were able to effectively integrate the extra charge delivered by the pulse with longer PPD, while the animals with poor neural survival were not. Using stimuli with equal charge, Ramekers et al. (2014) reported that SGN density and perikaryal area significantly predicted the PPD effect on the eCAP threshold, with larger PPD effects being observed in animals with lower SGN densities and smaller perikaryal areas. This indicated that the animals with poorer neural survival and smaller SGN cell bodies had a larger benefit from the increased temporal separation between the leading and lagging phases of the stimulus that arose from the change in PPD from 20 μs to 50 μs than the animals with better neural survival and larger SGN cell bodies. Therefore, the results from both studies indicate that the PPD effect on physiologic threshold is affected by the underlying neural condition.

2.1.3.2. Studies in human CI users: To date, only two studies have investigated the effect of increasing the PPD on the eCAP in human listeners (He et al., 2020a; Hughes, 2022). In their study, He et al. (2020a) compared eCAP thresholds, maximum eCAP amplitudes, and slopes of the eCAP AGF for stimuli with equal charge and PPDs ranging from 50 to 88 μs in two study groups: children with CND and children with normal-sized ANs. Despite trends of decreasing eCAP amplitude and increasing eCAP thresholds with increasing PPD for children with normal-sized ANs, there was not a statistically significant effect of PPD on any of the three eCAP parameters for either study group. Consistent with those results, Hughes (2022) reported a nonsignificant difference in the eCAP amplitude at different PPDs (Advanced Bionics: 27 and 32 μs, Cochlear Americas: 25 and 50 μs). However, Hughes (2022) reported a significant effect of PPD on eCAP threshold (in units of dB re: 1 nC) in both patients with Cochlear™ Nucleus® CIs and patients with Advanced Bionics devices. For both device manufacturers, lower eCAP thresholds were observed with shorter PPDs consistent with shorter pulses being more efficient and less prone to the leaky characteristics of the neural membrane. The apparent discrepancy in results of the PPD effect on eCAP threshold between He et al. (2020a) and Hughes (2022) can be explained by the range of PPDs tested in He et al. (2020a). As noted in He et al. (2020a), that study was limited to only four test PPDs (50, 67, 75 and 88 μs) due to the lack of measurable eCAPs at shorter PPDs in children with CND and the challenge of removing electrical artifact contamination from the eCAP recording at longer PPDs. However, eCAPs were able to be recorded at PPDs of 25 and 37 μs for children with normal-sized ANs. The eCAP thresholds measured in children with normal-sized ANs at six PPDs (25, 37, 50, 67, 75 and 88 μs) are shown in Figure 3B. The results of a linear mixed-effects model, with PPD as the fixed effect and ear/electrode as the random effect, demonstrated a significant effect of PPD on eCAP threshold ($F_{(5,522)} = 3.61$, $p = 0.003$). Overall, these results indicate that the eCAP threshold increases with increasing PPD for stimuli with equal charge and PPDs ranging from 25 to 88 μs. Taken together, the existing literature and data show that more charge is required to evoke an eCAP at longer PPDs. Finally, Hughes (2022) reported lower eCAP thresholds (in units of dB re: 1 μA) at longer PPDs, indicating that less current is needed to elicit an eCAP response at longer PPDs. There was approximately a 2.5% reduction in eCAP threshold as the PPD was increased from 27 to 32 μs in patients with Advanced Bionics devices and approximately a 11.7% reduction in eCAP threshold as the PPD was increased from 25 to 50 μs in patients with Cochlear™ Nucleus® CIs. The difference in threshold reduction between the CI manufacturers is expected due to the difference in magnitude of the PPD change (Advanced Bionics: 5 μs, Cochlear Americas: 25 μs).

2.1.3.3. Summary: For both animal models and human CI users, increasing the PPD with a constant pulse amplitude decreases the eCAP threshold because of the increase in total amount of electrical charge integrated by the neural membrane. The effect of increasing PPD with constant-charge stimuli on the eCAP is influenced by the IPG because of the increased temporal separation between the leading and lagging phases of a biphasic pulses. In animals, the effect of PPD on eCAP reflects underlying neural condition. Further studies are warranted to investigate the potential relationship between PPD effects and the underlying neural condition in human listeners.

2.1.4. Sensitivity to Changes in the Interphase Gap—Increasing the duration of the IPG for a biphasic stimulus increases the responsiveness of the AN to electrical stimulation because the action potential generated by the leading pulse is less susceptible to abolishment by the lagging pulse with the opposite phase (van den Honert & Mortimer, 1979; Shepherd & Javel, 1999). An action potential is *initiated* when the neural membrane reaches its firing threshold. However, an action potential cannot be *generated* if the cell is repolarized toward the resting potential during the time required to activate voltage-sensitive sodium ion channels (Bromm & Frankenhaeuser, 1968). Therefore, extending the time between the leading and lagging pulses with increased IPG boosts the probability of spike initiation (van den Honert & Mortimer 1979; Shepherd & Javel, 1999; Rubinstein et al., 2001). The effect of increasing the IPG is influenced by the integrative time constants of the neural membrane, which are affected by fiber diameter, myelination, and the kinetics of the voltage-gated sodium channels (Shepherd & Javel, 1997; Rubinstein et al., 2001; Resnick et al., 2018; Heshmat et al., 2020). Fiber diameter and myelination can decrease following SNHL (Leake & Hradek, 1988; Spoendlin & Schrott, 1989; Agterberg et al., 2008), which would affect the effectiveness of increasing the IPG on improving the probability of spike initiation at the AN. Therefore, the effect of increasing the IPG on the eCAP has been proposed to reflect the underlying neural condition of the AN.

2.1.4.1. Studies with animal models: Animal studies have repeatedly shown that increasing the duration of the IPG increases the responsiveness of the AN to electrical stimulation. This is demonstrated by lower eCAP thresholds (Prado-Guitierrez et al., 2006; Ramekers et al., 2014, 2015a, 2022; Vink et al., 2020) and larger eCAP amplitudes at longer IPGs with equal stimulation levels (Prado-Guitierrez et al., 2006; Ramekers et al., 2014, 2015a, 2022; Vink et al., 2020).

In animal studies, the sensitivity of the eCAP to changes in the IPG of biphasic pulses (i.e., IPG effect) has been reported to indicate SGN survival (Prado-Guitierrez et al., 2006; Ramekers et al., 2014, 2022). This has been shown by smaller changes in N1 latency (Ramekers et al., 2014, 2022) and larger differences in stimulation level required to evoke eCAP responses of equal amplitudes at different IPGs (i.e., stimulation level offsets; Prado-Guitierrez et al., 2006; Ramekers et al., 2014, 2022) with larger SGN cell size and/or higher SGN density. Ramekers et al. (2022) proposed that both results may reflect a shift in excitation preference from cathodic-first to cathodic-second biphasic stimuli that occurs simultaneously with deafness-induced SGN degeneration.

There are some discrepancies in results related to neural survival and the IPG effect on the slope of the eCAP AGF. Ramekers et al. (2014, 2022) showed a positive correlation between SGN density and the size of the IPG effect on the slope of the eCAP AGF, while Brochier et al. (2021b) provided results of a nonsignificant IPG effect using the data from Prado-Guitierrez et al. (2006). The reasons for these discrepancies are not well understood. However, there are some noticeable methodological differences between Prado-Guitierrez et al. (2006) and Ramekers et al. (2014, 2022). These differences include PPDs (104 μs vs 20-50 μs) and IPGs evaluated (8 and 58 μs vs 2.1 and 30 μs), stimulation mode (bipolar vs monopolar) and quantification of the eCAP amplitude (P2-N2 vs N1-P2). It should be pointed out that there is a significant interaction effect between the IPG and PPD on the

slope of the eCAP AGF because both factors increase the temporal separation between the leading and lagging phases of a biphasic pulses (Ramekers et al., 2014). Therefore, these differences in IPGs and PPDs may partially contribute to the apparent discrepancy in the results reported in these three studies.

2.1.4.2. Studies with human CI users: Studies with CI users have shown that longer IPGs increase the responsiveness of the AN to electrical stimulation. This is demonstrated by lower eCAP thresholds (Hughes et al. 2018; He et al., 2020b; Imsiecke et al., 2021), larger eCAP amplitudes at equal stimulation levels (Kim et al., 2010; Schvartz-Leyzac & Pfingst, 2016, 2018; Hughes et al. 2018; He et al., 2020b; Langner et al., 2021), and decreased N1 latencies (Skidmore & He, 2021). However, like the animal studies, findings regarding the effect of increasing the IPG on the slope of the eCAP AGF are conflicting. Schvartz-Leyzac & Pfingst (2016, 2018) reported significantly steeper slopes at longer IPGs, but Hughes et al. (2018) and Langner et al. (2021) did not find any difference in the slope at different IPGs. He et al. (2018) reported a significant IPG effect on the slope of the eCAP AGF when the slope was calculated using sigmoidal regression, but there was no significant IPG effect when the slope was calculated using linear regression. Imsiecke et al. (2021) reported a significant IPG effect on the slope when using the absolute slope (i.e., units of μV/nC), but not when using the slope normalized to the maximum eCAP amplitude (i.e., units of 1/nC). These studies highlight the difficulty in comparing results across studies when different methods and/or units were used to quantify the slope (Skidmore et al., 2022b; Yuan et al., 2022). As a result, whether there is any discrepancy in the IPG effect on the slope of the eCAP AGF across studies remains unknown and is difficult to determine based on the existing literature.

The results from the animal studies described above inspired several studies with human CI users to investigate the use of the IPG effect on eCAP parameters to predict neural survival. Consistent with the theories developed from the animal models, the IPG effect on several eCAP parameters is significantly different between children with CND and children with normal-sized ANs (He et al, 2020b; Skidmore & He, 2021). However, the magnitude and direction of differences in the IPG effect on eCAP parameters between the two patient populations were affected by the method in which the data were analyzed/quantified (Yuan et al., 2022). For example, the absolute difference in the linear slope at different IPGs was *smaller* for children with CND than children with normal-sized ANs, but the proportional difference in the linear slope was *larger* for children with CND than children with normal-sized ANs. Therefore, the method for quantifying the IPG effect has important implications for the interpretation of results. This has been highlighted in a few recent studies (Brochier et al., 2021a; Yuan et al., 2022; Takanen et al., 2022).

2.1.4.3. Summary: In both animal and human studies, increasing the duration of the IPG increases the responsiveness of the AN to electrical stimulation and results in lower eCAP thresholds and larger eCAP amplitudes. Results from studies with animal models, suggest that the IPG effect on eCAP parameters can be indicative of neural population size and/or health. Results from children with CND and children with normal-sized ANs suggest that the IPG effect on eCAP parameters primarily reflects neural survival. Simulation results

from studies using computational modeling techniques show conflicting information about the potential underlying neural condition that the IPG effect represents. For example, Brochier et al. (2021a) suggested that the stimulation level offset is reflective of central axon demyelination, as opposed to the number of surviving neurons. This is also supported by another recent modeling study which showed that the stimulation level offset (using the same method used by Brochier 2021a, b) was not sensitive to neural survival (Takanen et al., 2022). However, Takanen et al. (2022) showed in their modeling study that the absolute IPG effect on slope is indicative of neural survival, which agrees with results from animal studies (Ramekers et al., 2014, 2022) but disagrees with results from the modeling study by Brochier et al. (2021a). Interpreting these simulation results always requires caution because they have not been systematically validated using experimental data collected in human CI users. In addition, the computational models used in these studies were developed based on data measured in animals and depend on several underlying assumptions that have not been fully validated in human listeners. As a result, how applicable these simulation results are to human CI users remains unknown.

2.1.5. Sensitivity to Change in the Number of Phases—The number of phases included in a single-pulse stimulus affects the time course of current delivered to the AN. Consequently, the number of phases in the stimulus affects the spread of excitation (Bahmer & Baumann, 2016) and the site of action potential initiation in the target SGNs (Heshmat et al., 2021). The responsiveness of the AN to electrical stimulation with different numbers of phases has been measured in animal models (Shepherd & Javel, 1999; Miller et al., 1999a, 2001b; Macherey & Cazals, 2016) and human CI users (Bahmer & Baumann, 2013; Herrmann et al., 2021).

2.1.5.1. Studies in animal models: Results from animal studies indicate that the AN is more responsive to fewer phases in the single pulse (Shepherd & Javel, 1999; Miller et al., 1999a, 2001b; (Macherey & Cazals, 2016). Miller et al. (2001b) showed that 40 μs monophasic pulses produced lower thresholds than 40 μs/phase biphasic pulses using eCAP and single-fiber recordings in guinea pigs and cats. Guinea pigs showed a smaller difference in eCAP thresholds between monophasic and biphasic pulses than cats (Guinea pig: 1.7 dB difference, Cat: 3.4 dB difference), which might be due to the differences in cochlear anatomy between the two species (Miller et al., 2001b). Two other single-fiber studies with cats also reported firing thresholds that were approximately 4 dB lower for monophasic pulses than for biphasic pulses (Shepherd & Javel, 1999; Miller et al., 1999a). Additionally, Shepherd & Javel (1999) showed that the firing threshold was approximately 3-4 dB lower for biphasic pulses than triphasic pulses. Finally, Macherey and Cazals (2016) reported that triphasic pulses required 2.7 dB more current than biphasic pulses to evoke potentials of the same amplitude in the inferior colliculus.

2.1.5.2. Studies in human CI users: Electrical stimulation in human listeners is charge-balanced to prevent electrode damage and the production of neurotoxic agents at the surface of the CI electrode contacts (Brummer & Turner, 1975; Shepherd et al., 1991, 1999; Merrill et al., 2005). Therefore, monophasic pulses are not viable as stimuli in CI users. However, charge-balanced ‘pseudo-monophasic’ pulses consisting of a brief phase of one polarity

followed by a longer and lower-amplitude phase of the opposite polarity have been used in behavioral studies (van Wieringen et al., 2005; Macherey et al., 2006). These studies show that pseudo-monophasic pulses may be clinically beneficial for CI users by reducing power consumption, increasing dynamic range, and limiting channel interactions (van Wieringen et al., 2008). To date, no study has reported eCAP responses evoked by pseudo-monophasic pulses. Two physiologic studies have shown that triphasic pulses generate lower eCAP amplitudes and higher eCAP thresholds compared to biphasic pulses at equal charge levels (Bahmer & Baumann, 2013; Herrmann et al., 2021). However, triphasic stimulation may have clinical utility because the use of triphasic pulses significantly reduced facial nerve stimulation in CI users who experienced stimulus induced discomfort with biphasic pulses (Braun et al., 2019; Alhabib et al., 2021).

2.1.5.3. Summary: The effect of number of phases on the eCAP has not been systematically studied and remains poorly understood. The available literature in both animal models and human CI users shows that AN sensitivity to electrical stimulation decreases with increasing numbers of phases included in the single pulse stimulus.

2.2. Response Properties to Paired-Pulse Stimulation

Paired-pulse stimulation refers to the stimulation condition where two electrical pulses are presented in pairs with varied inter-pulse intervals (IPIs). This stimulation paradigm is also referred to as masker-probe stimulation when the IPI is long enough for the first pulse to induce a masking effect. Paired-pulse stimulation has been used to assess two temporal response properties of ANFs: facilitation and recovery from refractoriness (i.e., refractory recovery).

2.2.1. Facilitation—Facilitation refers to increased neural responsiveness to paired, subthreshold stimuli presented in rapid succession, as illustrated in Figure 4. This phenomenon has also been called sensitization (Dynes, 1996) or temporal summation (Cartee et al., 2000, 2006), but most studies have adopted the term facilitation in recent years (Cohen, 2009; Heffer et al., 2010; Karg et al., 2013; Ramekers et al., 2015a; Boulet et al., 2016; Hey et al., 2017; Tabibi et al., 2019). The proposed mechanisms underlying facilitation include capacitive charging of the neural membrane and residual sodium activation after the first stimulus (Boulet et al., 2016). Both mechanisms lead to increased facilitation at shorter IPIs (Dynes, 1996; Cartee et al., 2000, 2006). Additionally, the effects of these mechanisms may accumulate during pulse-train stimulation and further increase neural responsiveness (Saeedi et al., 2021).

2.2.1.1. Studies in animal models: To date, only three studies have investigated facilitation of the AN using eCAP measurements in animal models (Stypulkowski & van den Honert, 1984; Ramekers et al., 2015a, b). While not the primary focus of their study, Stypulkowski & van den Honert (1984) reported increased eCAP amplitudes at IPIs less than 150 μs due to facilitation in cats. Ramekers et al. (2015a, b) assessed facilitation in guinea pigs with normal hearing and deafened guinea pigs with various degrees of SGN loss. In all three study groups, Ramekers et al. (2015a) found that the relative contribution of the facilitation component in a two-component (i.e., facilitation and

refractory recovery) exponential recovery function (i.e., the facilitation amplitude constant) increased with stimulation level. The stimulation level did not affect the time window of facilitation (characterized by the facilitation time constant) for any of the three study groups. Ramekers et al. (2015b) did not investigate the stimulation level effect on facilitation. Both studies by Ramekers and colleagues reported that, on average, the facilitation amplitude constant was greatest for normal-hearing animals (group mean approximately 6.5) and lowest for the animals with severe SGN loss (group mean approximately 5.0). However, results of statistical analyses revealed no significant difference in facilitation amplitude constant between study groups (Ramekers et al., 2015a, b). Ramekers et al. (2015b) reported significantly larger facilitation time constants in normal hearing controls (group mean approximately 470 μs) than in guinea pigs deafened for 14 weeks (group mean approximately 270 μs). In contrast, there was not a significant group effect in facilitation time constant for the three study groups in Ramekers et al. (2015a) which consisted of guinea pigs deafened for 2 weeks or 6 weeks and normal hearing controls. Therefore, these results suggest that the loss of SGNs induced by prolonged deafness creates a weakened facilitation effect.

Single-fiber studies have reported facilitation effects in cats (Dynes, 1996; Cartee et al., 2000, 2006) and guinea pigs (Heffer et al., 2010). In cats, the facilitation effects were strongest at small IPIs (e.g., < 200 μs), but could be observed up to IPIs of 1 ms (Dynes, 1996; Cartee et al., 2000, 2006). Heffer et al. (2010) reported that single-fiber facilitation was weaker in chronically deafened guinea pigs with lower SGN density than in acutely deafened guinea pigs with greater SGN density. The results from Heffer et al. (2010) suggest that poorer neural survival is associated with weaker facilitation, presumably due to reduced current integration caused by demyelination (Koles & Rasminsky, 1972; Spoendlin, 1984). The trends in averaged eCAP results from Ramekers et al. (2015a, b) agree with this result, but the differences in study groups were not statistically significant. In addition to the difference between Heffer et al. (2010) and Ramekers et al. (2015a, b) in study design (i.e., single-fiber vs eCAP), the difference in IPGs (8 μs vs 30 μs) could also contribute to the differences in results between the studies because the IPG significantly impacts AN responsiveness to electrical stimulation (see Section 2.1.4 above). However, this remains a speculation because a possible interaction between facilitation strength and the IPG effect on the eCAP has not yet been investigated.

2.2.1.2. Studies in human CI users: Facilitation has been observed up to IPIs of 1 ms in human CI users (Cohen, 2009; Karg et al., 2013; Hey et al., 2017; Tabibi et al., 2019) and for any pulse polarity combination of biphasic pulses (Karg et al., 2013). The strongest facilitation effect is observed when the first pulse (i.e., conditioner/facilitator pulse) is near the eCAP threshold (Hey et al., 2017; Tabibi et al., 2019). Additionally, the facilitation strength (i.e., maximum facilitation amplitude) and speed (i.e., time constant) are not dependent on the intensity of the second (i.e., probe) pulse (Hey et al., 2017; Tabibi et al., 2019). Both observations are intuitive because facilitation is dependent on the residual excitability of the AN after a subthreshold pulse. Therefore, maximum facilitation would be expected at maximum *subthreshold* stimulation (i.e., immediately below threshold). The second pulse would simply need to be large enough to activate the neuron to its firing

threshold. This pulse could be small and still elicit an action potential if the neuron is near threshold after the first pulse. As the IPI grows, the neuron has more time to return to its resting potential, which decreases the facilitation strength.

The strength of facilitation varies between individual listeners (Cohen, 2009; Tabibi et al., 2019) and may reflect the underlying neural condition of the AN. Specifically, Tabibi et al. (2019) reported a positive correlation between the facilitation strength and the slope of the eCAP AGF, which likely indicates more and healthier ANFs (Cafarelli Dees et al., 2005; Ramekers et al., 2014; Pfingst et al., 2015a, b; Pfingst et al., 2017; Schvartz-Leyzac et al., 2019, Vink et al., 2020; Jahn & Arenberg, 2020a, b; Mussoi & Brown, 2020; Shader et al., 2020; Skidmore et al., 2022a).

2.2.1.3. Summary: Facilitation has been observed in both animal models and human CI users at IPIs up to 1 ms. The rate of facilitation decay with increasing IPI is not affected by the stimulation level. Additionally, results from animal models and human CI users suggest that stronger facilitation is associated with a greater abundance of functional ANFs. However, additional studies are warranted to verify this conclusion.

2.2.2. Refractory Recovery—Refractoriness refers to the decreased neural responsiveness following an action potential. It is a feature that enhances the precision of action potential timing (Avissar et al., 2013). The biological mechanism primarily responsible for this decreased responsiveness is the inactivation of the neuron's sodium channels caused by the previous action potential (Boulet et al., 2016), but other voltage-gated ion channels can influence the time-course of the refractory recovery (Negm & Bruce, 2014; Boulet & Bruce, 2017). The refractory process includes two stages: absolute and relative refractoriness. Absolute refractoriness refers to a status in which neurons are incapable of generating an action potential immediately after a previous stimulation. The time from the action potential until the neuron returns to a state in which it could generate another action potential with sufficient stimulation is called the absolute refractory period (ARP). After the ARP, the neuron progressively becomes more susceptible to generate an action potential until it returns to its normal excitability. The time interval from the end of the ARP to the normal threshold is called the relative refractory period (RRP). Both the ARP and the RRP can be estimated with the refractory recovery function (RRF). The RRF is obtained through a pair-pulse stimulation paradigm in which the IPI is systematically varied between the first (masker) pulse and the second (probe) pulse. As the IPI increases, the AN gradually recovers from the refractoriness induced by an action potential generated by the first pulse, which results in decreased thresholds and increased neural responses at longer IPIs. An illustration of the RRF is provided in Figure 4.

2.2.2.1 Studies with animal models: Most animal studies reporting estimates for the ARP and the RRP used single-fiber recordings (Dynes, 1996; Cartee et al., 2000; Miller et al., 2001a; Shepherd et al., 2004; Avissar et al., 2013), while only three animal studies used eCAPs to acquire these estimates (Stypulkowski & van den Honert, 1984, Ramekers et al., 2015a, b). Specifically, Stypulkowski & van den Honert (1984) reported ARPs to be approximately 0.3 - 0.4 ms in cats, and Ramekers et al. (2015a, b) reported ARPs to be approximately 0.4 – 0.8 ms in guinea pigs. Aside from the different species between

the study by Stypulkowski & van den Honert (1984) and the studies by Ramekers and colleagues, there was also a difference in the stimulus used. Specifically, Stypulkowski & van den Honert (1984) used 100 μs monophasic pulses while Ramekers et al. (2015a, b) used alternating polarity, biphasic pulses with 30 μs PPDs. Therefore, it is not certain if the longer ARPs reported in guinea pigs were due to differences in species or stimulation parameters. Animal studies with single-fiber recordings have reported average ARPs ranging from 0.3 to 0.7 ms in cats (Dynes, 1996; Miller et al., 2001a) and 0.7 to 0.9 in rats (Shepherd et al., 2004). Using the eCAP RRF, Ramekers et al. (2015a, b) reported refractory recovery time constants to be approximately 1.0 – 2.0 ms in guinea pigs. This would correspond to RRPs of approximately 3.0 – 6.0 ms, when estimating the RRP as three times the refractory recovery time constant (i.e., 95% recovery). Single-fiber studies have reported RRPs that range from approximately 0.4 to 2.0 ms in cats (Dynes, 1996; Cartee et al., 2000; Miller et al., 2001a). Therefore, estimated refractory periods vary substantially across animal species.

In addition to differences in estimates of refractory periods *across* species of animal models, differences in refractory periods *within* species have been reported depending on the physiological status of the AN. Specifically, Ramekers et al. (2015b) reported significantly longer ARPs in guinea pigs deafened for 14 weeks (group mean approximately 0.62 ms) than results measured in the normal hearing controls (group mean approximately 0.50 ms). Similarly, Zhou et al. (1995) reported in their eABR study that the surviving ANFs had significantly prolonged ARPs and RRPs in experimental mice with AN myelin deficiency compared to those in mice with normal hearing. In agreement with those results, a single-fiber study (Shepherd et al., 2004) reported significantly longer ARPs in long-term deafened rats (group median approximately 0.90 ms) compared to the normal hearing control group (group median approximately 0.65 ms).

2.2.2.2 Studies with human CI users: Several studies with CI users have reported estimated ARPs and RRPs for various patient populations. Overall, estimates for the ARP and the RRP time constant measured at the maximum comfort level (C level) are consistent across patient populations and typically fall within 0.2 to 0.6 ms and 0.6 to 1.4 ms, respectively (Pesch, 2005; Morsnowski et al., 2006; Hughes et al., 2012; Wiemes et al., 2016; He et al., 2018; Skidmore et al., 2021, 2022a). The one exception is that children with CND have significantly longer ARPs (mean: 1.31 ms, SD: 0.81 ms) that can last up to 3.42 ms (He et al., 2018). This result suggests that poor AN survival results in prolonged ARPs at the population level. In contrast, there were no differences in ARPs between children and adults with SNHL (Skidmore et al., 2021) or between middle-aged and elderly adults (Skidmore et al., 2022a). No difference in RRP time constants was reported between children with CND and children with normal-sized ANs (He et al., 2018), between children with auditory neuropathy spectrum disorder (ANSD) and children with SNHL (Fulmer et al., 2011; Kim et al., 2011), or between young to middle-aged adults and elderly adults (Lee et al., 2012). In their study, Botros and Psarros (2010) concluded that longer RRPs are associated with larger neural populations, which does not agree with the results presented in He et al. (2018). However, several considerations are important to highlight because this conclusion was based on results from a computational model of cat AN and comparing adult Cochlear Nucleus Freedom CI users with either contour or straight electrode arrays. First,

the computational model was developed using anatomical and physiological properties of the cat. As described above, there are likely many differences between cats and humans. Second, the computational model assumed that the eCAP amplitude was a direct predictor of perceived loudness, which is highly unlikely based on results reported by Kirby et al. (2012). Third, the assumption was made based on previous findings showing less spread of neural excitation in contour-array than in straight-array CI users (Cohen et al., 2003; Hughes & Abbas, 2006). However, the spread of neural excitation was not measured in Botros and Psarros (2010). Therefore, the assumed difference in neural population in their subject groups remains unverified. Based on the literature available it appears that the RRP is comparable across patient populations (Fulmer et al., 2011; Kim et al., 2011; Lee et al., 2012; He et al., 2018).

2.2.2.3. Summary: In general, there is no clear difference in estimated ARPs and RRPs between animal models and human CI users. The one exception is that ARPs for children with CND have been reported to be much longer than for animal models or for any other human patient population. As described before, histological results of human temporal bones show that children with CND have substantially fewer SGNs than age-matched controls (Nelson & Hinojosa, 2001; Chen et al., 2019; de Costa Monsanto et al., 2022). Therefore, these results suggest that prolonged ARPs are indicative of poor neural survival, which aligns with the results measured in animals with long-term deafness (Shepherd et al., 2004; Ramekers et al., 2015b). However, degeneration of the surviving ANFs may also be a contributing factor.

The RRF follows a decaying exponential function in both human CI users (e.g., Battmer et al., 2004; Morsnowski et al., 2006; Botros & Psarros, 2010; Fulmer et al., 2011; Wiemes et al., 2016; He et al., 2018; Tabibi et al., 2019; Skidmore et al., 2021, 2022a) and animal models (Zhou et al., 1995; Dynes, 1996; Cartee et al., 2000; Miller et al., 2001a; Ramekers et al., 2015a). Importantly, the speed of recovery from refractoriness is affected by stimulus level, with faster recovery at higher levels (Miller et al., 2001a; Shepherd et al. 2004; Battmer et al., 2004; Morsnowski et al., 2006; Ramekers et al., 2015a; Cohen, 2009; Botros & Psarros, 2010; Pesch et al., 2005; Tabibi et al., 2019). Therefore, comparisons of estimates of the ARP and RRP between species and patient populations may be confounded by the stimulation levels. Animal studies typically record responses at the same current levels for each subject (e.g., Ramekers et al., 2015a), while human studies typically record the eCAP RRF at an upper-comfort level to compare across subjects (e.g., Pesch, 2005; Morsnowski et al., 2006; Hughes et al., 2012; Wiemes et al., 2016; He et al., 2018; Skidmore et al., 2021, 2022a).

2.3. Response Properties to Pulse-Train Stimulation

Pulse-train stimulation refers to the condition in which the stimulus is a train of electrical pulses. The duration, carrier rate and amplitude envelope of pulse-train stimulation can be user-defined and vary across studies. eCAPs evoked by individual pulses of pulse-train stimulation can be used to assess peri-stimulus neural adaptation, recovery from neural adaptation and sensitivity to amplitude modulation cues at the level of the AN.

2.3.1. Neural Adaptation—Neural adaptation refers to a decrease in neural responsiveness to a constant stimulus over time. It can be induced by both acoustic and electrical stimulation presented at a suprathreshold or subthreshold level (e.g., Litvak et al., 2001; Meyer et al., 2007; Zhang et al., 2007; Miller et al., 2011). In acoustic hearing, depletion of neurotransmitters and desensitization of receptors at the synapse between the hair cell and auditory neuron have been proposed as the main neurophysiological mechanisms underlying neural adaptation (e.g., Goutman & Glowatzki, 2007). In electrical hearing, a persistent shift in intracellular and extracellular concentrations of sodium and potassium caused by pulsatile stimulation was initially proposed to be the underlying neurophysiological mechanism of neural adaptation (Litvak et al., 2001; Woo et al., 2009a, b, 2010). However, more recent modeling studies have shown that the dynamics of low-threshold potassium and hyperpolarization-activated cation channels that are known to be present in SGNs may be sufficient to explain the range of adaptation observed in electrical stimulation of AN fibers (Negm & Bruce, 2014; Boulet & Bruce, 2017).

Neural adaptation plays a crucial role in maximizing the efficiency of signal transmission by removing redundant information (Epping, 1990; Clague et al., 1997; Wark et al., 2007). In the auditory system, it plays an essential role in accurately encoding speech sounds. Specifically, rapid temporal and amplitude changes in the speech signal are represented in the discharge patterns of AN fibers for frequencies up to 5 kHz (Delgutte, 1980; Johnson, 1980; Delgutte & Kiang, 1984). When stimulated by a sustained stimulus, the firing rate of the AN rapidly peaks at the onset of sustained stimulation, and then gradually decreases (i.e., neural adaptation). Proper neural adaptation of the AN has been proposed to increase the temporal precision of speech onset representation, enhance the spectral contrast between successive speech segments, and encode phonetic contrasts based on characteristics of speech envelope cues (Delgutte, 1997). Neural adaptation of the AN to electrical stimulation can be studied using single-fiber recording techniques in animal models and electrophysiological measures of the eCAP in animal models and human CI users.

2.3.1.1. Studies in animal models: Neural adaptation of the electrically-stimulated AN is generally observed across time scales ranging from a few milliseconds to minutes (Moxon, 1971; Parkins, 1989; Litvak et al., 2001, 2003b; Zhang et al., 2007; Heffer et al., 2010; Hu et al., 2010; Miller et al., 2011). Spike rate adaptation measured using single-fiber recording, defined as the decreased neural excitability in response to ongoing stimulation, has been proposed to be one of the physiological mechanisms underlying neural adaptation. It can be quantified using a post-stimulus time histogram (PSTH) which is defined as spike count per time bin averaged over multiple trials and divided by the bin width. The PSTH shows that the spike rate of AN fibers is maximal at the onset of stimulation and gradually decreases over the course of 30-100 ms before reaching a stabilized low spike rate (Moxon, 1971; Hu et al., 2010). In cats, alternation in spike rate can be observed at 100 pulses per second (pps; Miller et al., 2011), which is presumably due to refractoriness (Javel, 1990). The amount of spike rate adaptation is greater at higher pulse rates and lower stimulation levels (Litvak et al., 2001; Heffer, 2010; Zhang et al., 2007; Miller et al., 2008; Hu et al., 2010). These rate and level effects on spike rate adaptation and the variability in the

strength of adaptation across ANFs are well explained by heterogeneity in half-maximal activation potentials of hyperpolarization-activated cyclic nucleotide-gated cation channels (Boulet & Bruce, 2017). The pulse rate effect can be partially overcome by increasing the stimulation level due to increased membrane excitation at higher stimulation levels (Zhang et al., 2007). In addition, the spike rate adaptation to sinusoidally amplitude-modulated pulse trains is generally lower than that to unmodulated pulse trains when the two trains are matched for onset spike rate (Hu et al., 2010). This difference can at least partially be attributed to the relatively low effective stimulation level of an amplitude modulated pulse train compared with that of an unmodulated pulse train. The time course of spike rate adaptation follows an exponential decay function (van den Honert & Stypulkowski, 1987; Javel et al., 1987; Litvak et al., 2001). Therefore, spike rate adaptation has historically been characterized by a two-component (i.e., a fast and a slow phase) exponential decaying function (Zhang et al., 2007). The time constants estimated for these two phases have been reported to be affected by pulse rates with smaller time constants estimated for higher pulse rates. Specifically, Zhang et al. (2007) reported that the medians of the fast and the slow phase time constant estimated for 250-pps pulse trains were 11 and 91 ms, respectively. These numbers were 7.7 and 70 ms for 5000-pps pulse trains. A more recent study by van Gendt et al. (2020) indicated that, rather than exponential adaptation, electrically-stimulated AN fibers tend to exhibit power-law adaptation, a phenomenon that has previously been demonstrated for acoustic stimulation of AN fibers (Zilany et al., 2009). Both the degree and the time course of spike rate adaptation vary among AN fibers in animal models (van den Honert & Stypulkowski, 1987; Dynes & Delgutte, 1992; Litvak, et al., 2001, 2003b; Zhang et al., 2007). For example, Dynes & Delgutte (1992) reported 30% normalized spike rate adaptation in approximately 25% of AN fibers, around 30-80% adaptation in 50% of AN fibers and more than 80% adaptation in the remaining 25% of AN fibers over a one-second period. These cross-fiber variations have been attributed to the difference in the ability of AN fibers to maintain homeostasis when metabolic demand increases (Litvak, et al., 2003b).

In addition to single-fiber recordings, neural adaptation of the AN has been assessed using the eCAP evoked by individual pulses of constant-amplitude pulse trains in cats (Abbas et al, 1997; Matsuoka et al., 2000a), rats (Haenggeli et al., 1998) and guinea pigs (Abbas et al, 1997; Matsuoka et al., 2000a, 2000b; Ramekers et al., 2015a, b; Vink et al., 2020). eCAP amplitudes for individual pulses of pulse trains measured in these animal models are relatively stable and have a negligible amount of adaptation over the course of stimulation for pulse rates up to 200 pps. For pulse rates of 400 pps and higher, eCAP amplitudes showed an abrupt decrease during the first 5 ms of stimulation, followed by a more gradual decrease lasting about 50 ms before reaching a plateau. These data trends suggest two phases of neural adaptation at the AN: a fast/rapid and a slow phase, which is consistent with the time course of spike rate adaptation. At pulse rates of 300 pps or higher, the eCAP amplitudes show an alternation between small and large amplitudes across pulse presentations (Abbas et al, 1997; Haenggeli et al., 1998; Matsuoka et al., 2000a; Ramekers et al., 2015a, b; Vink et al., 2020). Further increasing pulse rate diminishes the alternating pattern and results in an overall decrease in eCAP amplitude.

The alternating pattern in the eCAP amplitude has been proposed to be partially due to the refractory-recovery process occurring at the AN (Matsuoka et al., 2000a; Ramekers

et al., 2015a). Specifically, when the IPI is shorter than the refractory recovery time of SGNs, some neurons activated by the first pulse are not able to fire to the second pulse. Many of these neurons are sufficiently recovered to be excited by the third pulse. As a result, the eCAP amplitude is larger in response to the third pulse than to the second pulse. This refractory-recovery process occurs during the entire process of pulse-train stimulation, which results in a pattern of the eCAP amplitude alternation between smaller and larger amplitudes across pulse presentations (Wilson et al., 1997). This alternating pattern may also be affected by adaptation and relative spread of neural excitation among ANFs (van Gendt et al., 2019). In animal models, only the alternation between larger responses for odd-numbered pulses and smaller responses to even-numbered pulses is observed. The amount of alternation can be quantified by alternation depth, which is defined as the difference in normalized eCAP amplitude (re: the eCAP amplitude for the first pulse of the pulse train) between the largest and the smallest responses within each repeated group of responses. The alternation depth has been shown to be indicative of SGN survival in guinea pigs with larger alternation depths associated with poorer SGN survival (Ramekers et al., 2015a, b; Vink et al., 2020). The alternation starts at similar levels regardless of SGN survival but dampens more quickly for larger SGN populations (Vink et al., 2020), possibly because of lower across-cell synchronicity in larger SGN populations. This possibility is in line with results showing that the alternation depth decreases when applying Gaussian noise at approximately 30 dB below the eCAP threshold (Matsuoka et al., 2000a), which would cause more jitter among the SGN population.

The maximum alternation is expected to occur at the pulse rate that resonates with the refractory recovery period of the stimulated ANFs (Matsuoka et al., 2000a). In cats and guinea pigs, the maximum alternating depth is observed around 1000 - 1700 pps (Abbas et al., 1997; Ramekers et al., 2015a, 2015b; Vink et al., 2020). It can be affected by stimulation level with larger maximum alternation depths measured at higher stimulation levels for a given pulse rate (Matsuoka et al., 2000a). Matsuoka et al. (2000a) assessed the effect of stimulus polarity on neural adaptation pattern using the eCAP in cats and guinea pigs. They found that the maximum alternation depth was greater for cathodic-leading than anodic-leading biphasic pulses when measured at the same pulse rate and stimulation level in both animal models (Matsuoka et al., 2000a). Cats showed smaller maximum alternation depths than guinea pigs at the same stimulation level and pulse rate for both stimulus polarities (Matsuoka et al., 2000a). In addition, anodic-leading biphasic pulses caused a more gradual decline in response amplitude over the duration of the pulse train stimulation than cathodic-leading biphasic pulses. The maximum alternation depth also occurred at faster pulse rates for anodic than cathodic stimuli. These polarity effects were observed in cats but not in guinea pigs. This is consistent with a previous study showing differences in polarity effects on the eCAP between these two species (Miller et al., 1998). In addition, neural adaptation was not observed at pulse rates of 125 pps or lower at low stimulation levels and could be observed at higher pulse rates and stimulation levels in cats. In comparison, neural adaptation was not observed at pulse rates around 63 pps or lower and is less affected by stimulation level in guinea pigs. The anatomical differences in the cochlea, and differences in electrode geometry, neural properties, and neural survival, are

believed to account for these observed differences in eCAPs between cats and guinea pigs (Miller et al., 1999b; Matsuoka et al., 2000a).

The amount of neural adaptation can be quantified by the amount of reduction in normalized eCAP amplitude (re: the amplitude of the eCAP to the first pulse of the pulse train). The amount of neural adaptation increases with pulse rate (Abbas et al., 1997; Haenggeli et al., 1998) and the stimulation level of a masker pulse train (Killian et al., 1994), and decreases at higher probe levels (Nourski et al., 2007). For example, the eCAP amplitude at 1600 pps showed a reduction of approximately 60-80% compared to the same measure at 100 pps in rats (Haenggeli et al., 1998). The speed of neural adaptation of the AN assessed using the eCAP has not been evaluated using animal models.

2.3.1.2. Studies in human CI users: In human CI users, neural adaptation of the AN can also be assessed by measuring eCAPs to individual pulses of pulse trains (Wilson et al., 1997; Hay-McCutcheon et al., 2005; Clay & Brown, 2007; Hughes et al., 2012, 2014; Dhuldhoya, 2013; Zhang et al., 2013; He et al., 2016; Adel et al., 2017; Hughes & Laurello, 2017; Mussoi & Brown, 2019; He et al., 2022a). Similar to results obtained in animal models, eCAP amplitudes are relatively stable across individual pulses and show little or no adaptation at pulse rates of 200 pps or lower (Wilson et al., 1997). Increasing pulse rate results in a rapid decrease in the eCAP amplitudes in the first 5-10 ms after stimulus onset, followed by a more gradual decline up to 50 ms, before a steady state in amplitude is reached. At pulse rates of 400-2400 pps, eCAP responses demonstrate an alternating pattern of high and low amplitude as a function of pulse number (Wilson et al., 1997; Hughes et al., 2012; Zhang et al., 2013; He et al., 2016; He et al., 2022a). As pulse rate increases further, the alternating pattern diminishes and eCAPs stabilize with relatively small amplitudes across pulses. The pulse rate at which the alternating pattern ceases has been referred as the “stochastic rate” which typically occurs between 900 pps and 3500 pps and can increase at higher stimulation levels (Hughes et al., 2012; Hughes & Laurello, 2017).

In human CI users, eCAP amplitudes can alternate between large and small for odd- (even-) and even- (odd)-numbered pulses (Wilson et al., 1997; Hay-McCutcheon et al., 2005; Hughes et al., 2012; Zhang et al., 2013; He et al., 2016). More complicated alternating patterns, including triplet, quadruplet, quintuplet and sextuplet patterns (i.e., increase and decrease in amplitude that repeat every three, four, five or six responses), have also been reported (Wilson et al., 1997; Hay-McCutcheon et al., 2005; Hughes et al., 2012; He et al., 2016). These complicated alternating patterns are presumably due to variations in refractory recovery time across ANFs. The alternation depth increases as the stimulus level increases (Hughes & Laurello, 2017). The pulse rate at which the maximum alternation depth is observed occurs most often between 900 and 1800 pps but varies widely across individuals and electrode locations within individual CI users (Hughes et al., 2012; He et al., 2016; Hughes & Laurello, 2017).

The amount of neural adaptation has been estimated by comparing amplitudes of eCAPs elicited by individual pulses of a pulse train to the pre-adaptation eCAP amplitude (Hay-McCutcheon et al., 2005; Hughes et al., 2012; He et al., 2016, 2022a). The pre-adaptation eCAP amplitude can be quantified as the eCAP amplitude elicited by the first pulse of

the same pulse train (Hay-McCutcheon et al., 2005; Hughes et al., 2012; He et al., 2016) or by a single pulse presented at the same stimulation level as that of the pulse train (He et al., 2022a). Greater neural adaptation has been observed at higher pulse rates, lower stimulation levels and longer durations of stimulation (Wilson et al., 1997; Hughes et al., 2012; McKay et al., 2013; He et al., 2016; Hughes & Laurello, 2017; He et al., 2022a). For example, He et al. (2022a) reported that the mean amount of neural adaptation, as quantified by the percentage of reduction in normalized eCAP amplitude, measured for a 500-pps pulse train within the first 5 ms, around 50 ms, and near 100 ms was 12.46%, 21.07% and 23.91%, respectively. In comparison, the mean amount of neural adaptation measured for a 2400-pps pulse train within the first 5 ms, around 50 ms, and near 100 ms was 56.25%, 68.34% and 75.69%, respectively. Unfortunately, directly comparing the amount of neural adaptation reported across studies is challenging due to the difference in pulse rate, stimulation level, duration of stimulation, and method for quantifying the amount of neural adaptation used in different studies. He et al. (2016) found that children with ANSD had greater neural adaptation than children with idiopathic SNHL, especially for longer durations of stimulation. These results suggest that the amount neural adaptation can be affected by etiology of hearing loss. At a given pulse rate and stimulation level, the amount of neural adaptation varies substantially among CI users and across electrode locations within individual CI users (Hay-McCutcheon et al., 2005, Hughes et al., 2012; He et al., 2016; Hughes & Laurello, 2017). These variations cannot be predicted based on the location of the electrode within the cochlea (Hay-McCutcheon et al., 2005). It has been shown that the amount of neural adaptation of the AN is not associated with behavioral measures of temporal integration, pitch perception, gap detection threshold or speech perception scores (Hay-McCutcheon et al., 2005; McKay et al., 2013; Zhang et al., 2013; Hughes et al., 2014; Huarte et al., 2014).

Compared to the amount of neural adaptation, the speed of neural adaptation is understudied and less well understood. To date, it has only been investigated by He et al. (2022a). They found that the time course of neural adaptation of the AN in human CI users consisted of a rapid phase followed by a slow phase, which is consistent with results of single-fiber recordings in animal models (van den Honert, & Stypulkowski, 1987; Javel et al., 1987; Litvak et al., 2001; Zhang et al., 2007). As noted above, neural adaptation may be better described by a power law function (van Gendt et al., 2020). Time constants estimated using a power law function for results reported in He et al. (2022a) are listed in Table 1. These data clearly showed that the speed of neural adaptation of the AN was affected by the pulse rate, with higher pulse rates leading to faster neural adaptation (He et al., 2022a). Unfortunately, these data cannot be directly compared to the time constants estimated using an exponential function in cats from the study by Zhang et al. (2007).

To date, the association between neural adaptation of the AN and speech perception performance in human CI users has only been investigated in one study (He et al., 2022c). Their results showed that negligible or weak and nonsignificant correlations between Consonant-Nucleus-Consonant (CNC) word scores measured in quiet and in speech-shaped noise at a signal-to-noise ratio of +10 dB and the amount or the speed of neural adaptation of the AN.

2.3.1.3. Summary: In both animal models and human CI users, neural adaptation of the AN can be induced by electrical pulse trains with constant amplitude and pulse rates of 300 pps or higher. Overall, the amount and the speed of neural adaptation increase as pulse rate and stimulation level of masker pulse train increase. The reduction in neural response, quantified using either spike rate or eCAP amplitude, is rapid in the first few milliseconds and becomes relatively slow afterwards before reaching an asymptote. An alternating pattern in eCAP amplitude reduction can be observed at pulse rates of 400 pps or higher. The amount and the time course of adaptation varies across ANFs, animals and human CI users.

Despite these similarities in results recorded in different species, between-species differences in study results are also apparent. For example, stimulus polarity impacts certain aspects of neural adaptation of the AN in cats but not in guinea pigs (Matsuoka et al., 2000a). More importantly, the alternation is less robust in animal models than in human CI users (Abbas et al., 1997; Haenggeli et al., 1998).

2.3.2. Neural Adaptation Recovery—Recovery from neural adaptation caused by prior stimulation (i.e., neural adaptation recovery) at the level of the AN has been proposed to be important for neural representation of rapid onset transients in speech (Delgutte, 1997). Deficient neural adaptation recovery can compromise neural representation of speech envelope features (e.g., word onset and syllabic cues) (Jeng et al., 2009; Jahn et al., 2021), which leads to poor speech perception outcomes (He et al., 2022c). Neural adaptation recovery of the electrically stimulated AN can be studied using single-fiber recording technique in animal models (Miller et al., 2011). It can also be studied by measuring the eCAP evoked by a probe pulse with a preceding pulse-train masker at different masker probe intervals (MPIs) in animal models (Killian et al., 1994; Abbas et al., 1997; Nourski et al., 2007), as well as in human CI users (Dhuldhoya, 2013; Adel et al., 2017; Mussoi & Brown, 2019; He et al., 2022b). Compared with neural adaptation, neural adaptation recovery of the AN is less well-understood.

2.3.2.1. Studies in animal models: Animal models used to study neural adaptation recovery of the AN include cats (Abbas et al., 1997; Miller et al., 2009, 2011) and guinea pigs (Killian et al., 1994; Abbas et al., 1997; Nourski et al., 2007). In cats, results of single-fiber recordings show that temporal jitter recovers approximately 20 ms after masker offset. The recovery shows an initial rapid phase followed by a slow phase (Miller et al., 2009). In comparison, spike rate recovery is slow and relatively monotonic (Miller et al., 2009). These response properties largely recover to baseline approximately 100-200 ms after masker offset (Miller et al., 2009). Despite considerable variations in the amount of adaptation recovery across ANFs, using higher masker levels results in reduced adaptation recovery (Miller et al., 2011). For a fixed stimulation level, the amount and the speed of adaptation recovery depend on the pulse rate of the masker. For example, less and slower adaptation recovery is measured for a 5000-pps pulse-train masker than that measured for a 250-pps pulse-train masker (Miller et al., 2011).

Results of studies using eCAP recordings show that neural adaptation recovery of the AN is affected by stimulation levels of both masker and probe stimuli, masker duration and survival of SGNs (Killian et al., 1994; Abbas et al., 1997; Nourski et al., 2007). Specifically,

the amount of adaptation recovery reduces at higher masker and probe stimulation levels in guinea pigs (Killian et al., 1994). Using higher masker and lower probe current levels and longer duration of masker stimulation results in slower neural adaptation recovery in both cats and guinea pigs (Killian et al., 1994; Abbas et al., 1997). The adaptation recovery time measured in cats and guinea pigs in different studies vary from 10 ms to up to 900 ms (Killian et al., 1994; Abbas et al., 1997). Such a large range is due to the difference in eCAP testing paradigm, stimulation level and duration of masker pulse-trains used to assess adaptation recovery at the AN, as well as the hearing status of animal models among these studies.

Killian et al. (1994) and Nourski et al. (2007) reported that the time course of eCAP adaptation recovery could be monotonic or nonmonotonic depending on the stimulation levels of the masker pulse-train and the probe pulse, and the duration of the masker pulse-train. Results of these two studies showed that recovery from neural adaptation caused by lower-level maskers with shorter durations (e.g., 100 ms) typically followed a monotonic pattern. Using higher masker levels and longer masker durations (e.g., 300 ms) resulted in a non-monotonic recovery pattern (Killian et al., 1994; Nourski et al., 2007). The non-monotonic adaptation recovery pattern could consist of up to three phases: an initial rapid recovery within several milliseconds after the masker offset, a brief decline, and finally a slow recovery over several hundred milliseconds (Nourski et al., 2007). The differences in time course and sensitivity of temporal jitter recovery and spike rate recovery of ANFs have been proposed to partially account for this nonmonotonic recovery pattern (Miller et al., 2009). The characteristics of neural adaptation recovery of the AN is not affected by the presence of functional hair cells (Killian et al., 1994; Nourski et al., 2007) or the type of masker stimulation (acoustic vs electrical, Nourski et al., 2007).

2.3.2.2. Studies in human CI users: In human CI users, adaptation recovery of the AN has been evaluated by measuring the eCAP evoked by a probe pulse with a preceding pulse-train masker at different MPIs in four studies (Dhuldhoya, 2013; Adel et al., 2017; Mussoi & Brown, 2019; He et al., 2022b). Results of these studies showed that the time course of recovery could be monotonic or non-monotonic with up to three phases depending on the stimulation levels of the probe pulse and the pulse-train masker. The monotonic functions and the phases of the non-monotonic functions reported in these studies with human CI users are consistent with results recorded in animal models (Killian et al., 1994; Nourski et al., 2007). The number of adaptation recovery patterns with all three phases increases at higher pulse rates but is not affected by electrode location within the cochlea (He et al., 2022b).

Based on the number of phases included, He et al. (2022b) classified adaptation recovery patterns observed in their study into three types, as illustrated in Figure 5. The Type I pattern consists of an initial rapid increase followed by a slow increase in the eCAP amplitude. The Type II pattern consists of a rapid decrease followed by a slow increase of the eCAP amplitude. The Type III pattern includes an initial rapid increase followed by a rapid decrease and a second slow increase of the eCAP amplitude. The potential neurophysiological mechanisms underlying the initial rapid increase and the following rapid decrease in the eCAP amplitude are increased firing synchrony among ANFs (Nourski et

al., 2007; He et al., 2022b) and the decay of the facilitatory effect (Miller et al., 2011), respectively. Another alternative neurophysiological mechanism underlying the initial rapid increase in the eCAP amplitude is the integration of neural excitation across multiple pulses via the residual partial-depolarization mechanism (He et al., 2022b). The following decaying component can be a result of the combined effects of reduced facilitation, neural adaptation, accommodation (i.e., subthreshold adaptation), relative refractoriness, and neural adaptation recovery at the level of the AN (He et al., 2022b). The final slow recovery component reflects neural adaptation recovery (Nourski et al., 2007; Miller et al., 2011; He et al., 2022b).

The speed of adaptation recovery measured in human CI users has been quantified using the logistic function (Mussoi & Brown, 2019), or the exponential function with either one component or up to three components (Adel et al., 2017; Dhuldhoya, 2013; He et al., 2022b). In addition, study participants and pulse-train maskers differ among studies. These differences make it challenging to directly compare the speed of adaptation recovery across studies. Despite this challenge, results of these studies consistently showed substantial variations in the speed of neural adaptation recovery among CI users (Adel et al., 2017; He et al., 2022b). The speed of adaptation recovery is affected by stimulation levels of the masker and the probe pulse, with faster neural adaptation recovery for lower masker and higher probe stimulation levels. These results are consistent with that reported in animal models (Killian et al., 1994; Abbas et al., 1997). The speed of adaptation recovery is also affected by pulse rate. Adel et al. (2017) reported slower recovery from neural adaptation caused by the 5000 pps pulse-train masker compared to the 250 pps pulse-train masker, which is consistent with the results measured in guinea pigs (Miller et al., 2011). However, He et al. (2022b) reported a nonsignificant effect of pulse rate on the speed of adaptation recovery for a pulse rate range of 500-2400 pps. Therefore, this pulse rate effect may only be observed for large differences in pulse rate. The effect of advanced age on the speed of adaptation recovery has not been consistently reported in the literature. While Mussoi & Brown (2019) found that advanced age was associated with slower neural adaptation recovery of the AN, He et al. (2022b) reported a nonsignificant effect of advanced age on neural adaptation recovery process. However, the number of study participants who were younger than 40 years of age tested in He et al. (2022b) is limited, which might have precluded a thorough evaluation of the aging effect on the neural adaptation recovery process in their study. In addition, differences in methods used to assess and quantify neural adaptation recovery might have partially contributed to this discrepancy in aging effect reported in these two studies.

The amount of adaptation recovery of the AN in human CI users has only been investigated in He et al. (2022b). It was quantified by comparing the eCAP amplitude measured at the longest MPI tested to the eCAP amplitude measured for the single-pulse stimulus presented at the same stimulation level. Their results showed that the amount of neural adaptation recovery was affected by pulse rate with less adaptation recovery observed at higher pulse rates. This result is likely due to increased neural adaptation at higher pulse rates (He et al., 2022a). Thus, smaller eCAP amplitudes would be expected at a specified MPI for higher pulse rates even if the rate of recovery were not affected by pulse rate (He et al., 2022b). In addition, the amount of neural adaptation recovery varied for different adaptation recovery

patterns but was not affected by electrode location within the cochlea. Regardless of pattern type, adaptation recovery remains incomplete at an MPI up to 256 ms in many CI users (Dhuldhoya, 2013; He et al., 2022b).

Two studies have assessed the association between neural adaptation recovery of the AN and speech perception performance (Mussoi & Brown, 2019; He et al., 2022c). Both Mussoi & Brown (2019) and He et al. (2022c) reported a nonsignificant correlation between the *amount* of neural adaptation recovery of the AN and speech perception scores. In contrast, the *speed* of adaptation recovery accounted for 14.1% of variability in CNC word scores measured in quiet and 16.7% of variability in CNC word scores measured in noise (He et al., 2022c).

2.3.2.3. Summary: Results measured in different animal models and human CI users show some consistencies. Specifically, the adaptation recovery process substantially varies among ANFs in experimental animals and human CI users. In both animal models and human CI users, adaptation recovery can remain incomplete at an MPI up to at least 250 ms and is affected by pulse rate. In addition, the speed of neural adaptation recovery measured in different species depends on stimulation levels of the masker and the probe pulse. Finally, non-monotonic adaptation recovery patterns are observed in different animal models, as well as in human CI users.

A potential discrepancy in results measured in animal models and human CI users is the speed of adaptation recovery. Figure 6 shows the means and standard deviations of time constants of adaptation recovery measured in human CI users by He et al. (2022b) and in guinea pigs by Nourski et al. (2007). These time constants were estimated using similar mathematical models. In general, the mean time constants measured in human CI users are much shorter (less than 60 ms) than those measured in guinea pigs (i.e., 120 ms). It seems unlikely that such a large difference in the speed of adaptation recovery could be fully accounted for by the difference in pulse rate of masker pulse trains used in these two studies. Differences between Nourski et al. (2007) and He et al. (2022b) other than species and pulse rate include duration of stimulation (400 ms vs 100 ms), MPIs evaluated (up to 400 ms vs up to 256 ms), and eCAP amplitude normalization before function fitting (re: eCAP amplitude in response to a single pulse vs re: eCAP amplitude measured with an MPI of 256 ms). However, it remains unknown how these differences might affect the speed of adaptation recovery. Certainly, the amount of neural adaptation preceding adaptation recovery is affected by pulse rate and stimulation duration (Wilson et al., 1997; Abbas et al, 1997; Haenggeli et al., 1998; Hughes et al., 2012; McKay et al., 2013; He et al., 2016; Hughes & Laurello, 2017; He et al., 2022a), which could be anticipated to potentially influence the speed of adaptation recovery. However, He et al. (2022c) reported that there was no correlation between the amount of neural adaptation and the speed of adaptation recovery measured at the same electrode location. Therefore, factors accounting for the difference in speed of adaptation recovery between Nourski et al. (2007) and He et al. (2022b) are not entirely clear. To date, recovery from neural adaptation has not been simulated in biophysical or phenomenological models.

2.3.3. Amplitude Modulation Sensitivity—For programming strategies that are based on the continuous interleaved sampling strategy (Wilson et al., 1991), speech envelope information is extracted and used to amplitude-modulate trains of biphasic pulses that are delivered by CI electrodes. Electrical stimuli delivered by the CI are first encoded by the AN, before they can be transmitted to and processed by higher-level neural structures. Therefore, the capability of the AN to faithfully encode and transmit amplitude modulation (AM) cues should theoretically be important for CI outcomes.

AN encoding of AM cues can be studied using single-fiber and eCAP recordings in animal models (Hartmann et al., 1984; van den Honert & Stypulkowski, 1987; Dynes & Delgutte, 1992; Litvak et al., 2001, 2003a; Abbas et al., 1997, 2003; Runge-Samuelson et al., 2004; Jeng et al., 2009; Hu et al., 2010). In human CI users, it can only be investigated using eCAP measurements (Wilson et al., 1997; Tejani et al., 2017; Riggs et al., 2021).

2.3.2.1. Studies in animal models: Animal models used to study AN encoding of AM cues include cats (Hartmann et al., 1984; van den Honert & Stypulkowski, 1987; Dynes & Delgutte, 1992; Abbas et al., 1997, 2003; Litvak et al., 2001, 2003a; Runge-Samuelson et al., 2004; Hu et al., 2010), guinea pigs (Abbas et al., 1997, 2003; Runge-Samuelson et al., 2004; Jeng et al., 2009) and squirrel monkeys (Parkins, 1989).

Results of single-fiber recordings revealed a good sensitivity of AN fibers to AM cues. For example, the PSTHs for a 4800-5000 pps carrier pulse train with a sinusoidal AM rate of 400 Hz and a modulation depth of 0.5-1% are nearly sinusoidal in shape, which suggests that the AN firing pattern can follow the details of the sinusoidally-modulated waveform at these small modulation depths (Litvak et al., 2001, 2003a). At the onset of modulation, ANFs show an increase in averaged discharge rate and this increase is not due to changes in stimulation level (Litvak et al., 2001). ANFs phase-lock to both phases of the stimulus with one preferential phase that elicits the response at the threshold level. The response to the second phase can only be elicited at suprathreshold levels (Parkins, 1989). As a result, ANFs tend to discharge once during the preferential phase for every stimulus cycle in a precisely phase-locked manner at low AM rates (i.e., 500 Hz or lower) and at a threshold or a relatively low suprathreshold level (e.g., 6-10 dB above threshold) (Hartmann et al., 1984; van den Honert & Stypulkowski, 1987; Parkins, 1989). The degree to which ANFs phase lock to the periodic modulation of the stimulus amplitude improves over the time course of stimulation for AM rates up to 500 Hz (Hu et al., 2010). This regularity decreases at higher stimulation levels and higher AM rates. Specifically, ANFs can discharge during the opposite phase of the stimulus cycle and even discharge multiple times during one half-cycle at high stimulation levels (Hartmann et al., 1984; van den Honert & Stypulkowski, 1987; Parkins, 1989). The PSTHs measured for high AM rates (i.e., 4-10 kHz) only roughly follow a sinusoidal shape, which indicates that discharges are moderately phase-locked to the stimulus. A sinusoidally amplitude modulated (SAM) electrical stimulus with an AM rate of 100 Hz has been reported to be the most effective AM stimulus in evoking responses from ANFs (Hartmann et al.,1984; van den Honert & Stypulkowski, 1987). In addition to AM rate and stimulation level, modulation depth is another factor affecting the degree of phase locking to the stimulus of ANFs, with larger modulation depths associated with more precise phase locking (Litvak et al., 2001). Results of these studies also revealed considerable

variability among ANFs in the degree of phase-locking to the stimulus, especially for AM rates of 3 kHz or higher. In addition, how phase locking capability changes with AM rate varies substantially among ANFs. While the decline in phase-locking capability at higher AM rates is monotonic in some fibers, it can be nonmonotonic in other fibers.

In cats and guinea pigs, eCAPs can be evoked using AM pulse trains at AM rates of up to 1600 Hz using a 5000-pps carrier (Abbas et al., 1997). At AM rates of 50-400 Hz, the AN can encode modulation depths as small as 1%. With other stimulus parameters fixed, eCAPs increase in amplitude with AM rate up to 1000 Hz (Abbas et al., 1997), and with the presence of a low-level, high-rate conditioning pulse train (Runge-Samuelson et al., 2004). The recorded eCAPs show variations in amplitude, with smaller amplitudes measured at the valleys and larger amplitudes recorded at the peaks of the AM train. At low modulation depths and/or low AM rates (i.e., 200 Hz or lower), this eCAP amplitude pattern approximately follows the periodicity of the modulation waveform. At high modulation depths and/or high AM rates, the pattern does not always follow the detailed pattern of stimulus pulse amplitudes and becomes distorted from that of the stimulus envelope (Abbas et al., 1997; Jeng et al., 2009). The distortion typically shows as a phase shift (lead) relative to the stimulus, which suggests a degradation in the ability of AN fibers to encode stimulus modulations (Abbas et al., 2003; Jeng et al., 2009). This distortion is more robust at higher stimulation levels (Jeng et al., 2009). Nonlinear growth of the eCAP amplitude, adaptation, and refractoriness of the AN have been proposed to account for this phase-lead distortion (Jeng et al., 2009). The modulated response amplitude (MRA) has been used to quantify the strength of AM coding at the AN (Abbas et al., 2003; Jeng et al., 2009). It is defined as the difference in eCAP amplitudes measured at the peak and the valley of the AM stimulus over the same modulation cycle, as illustrated in Figure 7. Jeng et al. (2009) showed that the increment in the MRA was compressive in nature, with smaller increments measured for higher modulation depths. Temporal properties (e.g., refractoriness and adaptation) of the AN have been proposed to account for this compressive growth of the MRA. In addition, the MRA increases nonmonotonically as the AM rate increases up to 300 Hz for a 1000 pps carrier and up to 800 Hz for a 5000 pps carrier.

2.3.3.2. Studies in human CI users: To date, two studies have investigated AN encoding of AM cues in human CI users (Tejani et al., 2017; Riggs et al., 2021). Tejani et al. (2017) measured eCAPs evoked by each pulse over one modulation cycle of a 4000 pps, SAM pulse train with AM rates of 125, 250, 500 and 1000 Hz at one basal, one middle and one apical electrode location. Their results showed that eCAP amplitudes generally followed a sinusoidal pattern. In some but not all study participants, the phase-lead distortion in the eCAP amplitude pattern was observed. The MRA, which was defined as the difference in the maximum and the minimum eCAP amplitudes over one modulation cycle, increased with modulation depth and AM rate. These results are consistent with those reported in animal models (Abbas et al., 2003; Jeng et al., 2009). In addition, they found a significant, negative correlation between MRAs and psychophysical modulation detection thresholds (MDTs) for all except the 1000 Hz AM rate, which suggested a central limitation to processing of modulated stimuli. Both MRA and MDT were affected by electrode location, with larger MRAs and lower MDTs measured at more apical electrode locations. Using a 2000 pps,

SAM pulse train with AM rates of 20, 40, 100 and 200 Hz, Riggs et al. (2021) assessed AN encoding of AM at up to seven electrode locations across the electrode array. In their study, the AN sensitivity to AM was quantified using the modulated response amplitude ratio (MRAR) which was defined as the ratio of the difference in the maximum and the minimum eCAP amplitude measured for the AM pulse train to that measured for the single pulse, as illustrated in Figure 7. Greater MRARs indicate better sensitivity to AM cues. Overall, their results showed that AN sensitivity to AM cues was negatively affected by advanced age, which is presumably due to age-related decline in AN health (e.g., Wu et al., 2019), and reflects poorer temporal processing with aging. Similar to results of Tejani et al. (2017), a phase shift (lead) in eCAP amplitude pattern was observed in some but not all recordings (around 34% of all recordings) with more phase shift observed at higher AM rates. In addition, MRARs measured at the 200 Hz AM rate were significantly higher than those measured at all other AM rates, which is consistent with that reported in Tejani et al. (2017). In contrast to the reported better AM sensitivities at more apical electrode locations in Tejani et al. (2017), Riggs et al. (2021) reported better AN sensitivity to AM cues at more basal electrode locations. As explained in Riggs et al. (2021), results of these two studies do not necessarily contradict each other due to differences in the methods used to quantify the AN sensitivity to AM cues (MRA vs MRAR) and the AM rates investigated in these two studies.

2.3.3.3. Summary: To date, results measured in different animal models and human CI users for AN sensitivity to AM cues are largely consistent. For example, larger eCAP amplitudes to AM pulse trains are recorded for higher AM rates and greater modulation depths in both animal models and human CI users (Abbas et al., 2003; Jeng et al., 2009; Tejani et al., 2017; Riggs et al., 2021). The phase-lead distortion in eCAP amplitude pattern is observed in both animal models and some human CI users (Abbas et al., 2003; Jeng et al., 2009; Tejani et al., 2017; Riggs et al., 2021). However, these consistencies cannot be interpreted/used as the evidence supporting the notion that AM encoding at the AN is comparable across species, primarily due to the limited studies/knowledge in human CI users. To date, ANF firing patterns to modulated pulse trains cannot be accurately simulated using any existing biophysical or phenomenological models, which represents a knowledge gap that needs to be addressed.

3. CONCLUSIONS

Neural response properties of ANFs to electrical stimulation are affected by many factors, including stimulating and recording parameters (e.g., stimulation current level, pulse rate, stimulation duration, recording electrode location, etc.), quantification method (e.g., fitting function, normalization process, etc.), and study participant (different animal models vs human listeners). It is critical to take these crucial factors into consideration in study design, results interpretation, and comparison across multiple studies. Despite decades of research in animal models and human listeners, some areas remain controversial, poorly understood, or even completely unknown. For example, whether the difference in polarity sensitivity can be used to assess peripheral axon degeneration remains controversial. The effect of changing the number of pulse phases on neural response properties of healthy or impaired ANFs

remains poorly understood due to the limited available literature. Furthermore, the field currently lacks *in vivo* tools to differentially quantify lack of neural survival vs degeneration of surviving ANFs in human CI users. As a result, their specific effect on neural encoding of electrical stimulation in the AN remains completely unknown. Further studies are definitely warranted to address these knowledge gaps.

Computational models of ANFs can provide insightful mechanistic information about how neural encoding of electrical stimulation in the AN is affected by different types and degrees of pathological insults to ANFs, which is crucial information that cannot be directly assessed in human CI users. However, this review clearly demonstrates that information and knowledge gained from animal models cannot be simply translated to human listeners. This is partly due to some important differences in response properties of the AN. Some of these differences are quantitative in nature (e.g., the time course of recovery from neural adaptation) while others are more qualitative in nature (e.g., the differences in responsiveness to anodic vs cathodic stimulation and alternation patterns in response amplitudes to pulse train stimuli). At this point, exclusively including physiological parameters recorded in human listeners in various computational models is still not feasible due to the lack of information about different parameters of ion channels (e.g., ion channel type, kinetics, densities, etc.) involved in action potential generation, as well as data of morphometric characteristics and biophysical properties of different auditory neural structures in humans. However, it is critical to take the species differences into consideration when developing computational models for simulating response patterns of the electrically stimulated AN in human listeners. Additionally, these models should be verified with electrophysiological data measured in human CI users.

Source of Funding:

This work was supported by the R01 grant from NIDCD/NIGMS (1R01 DC016038), the R01 grant from NIDCD (1R01 DC017846) and the R21 grant from NIDCD (R21 DC019458) to Shuman He. Dyan Ramekers received funding from MED-EL GmbH, Innsbruck, Austria. Ian C. Bruce was supported by NSERC Discovery Grant #RGPIN-2018-05778.

ABBREVIATIONS

ARP	absolute refractory period
AGF	amplitude growth function
AM	amplitude modulation
AN	auditory nerve
ANF	auditory nerve fiber
ANSD	auditory neuropathy spectrum disorder
eCAP	electrically evoked compound action potential
eABR	electrically evoked auditory brainstem response
CI	cochlear implant

CNC	Consonant-Nucleus-Consonant
CND	cochlear nerve deficiency
IPG	interphase gap
IPI	inter-pulse interval
MDT	modulation detection threshold
MPI	masker probe interval
MRA	modulated response amplitude
MRAR	modulated response amplitude ratio
nC	nanocoulombs
N1	first negative peak in eCAP waveform
N2	second negative peak in eCAP waveform
P1	first positive peak in eCAP waveform
P2	second positive peak in eCAP waveform
PPD	pulse phase duration
pps	pulses per second
PSTH	post-stimulus time histogram
RRF	refractory recovery function
RRP	relative refractory period
SAM	sinusoidally amplitude modulated
SGN	spiral ganglion neuron
SNHL	sensorineural hearing loss

REFERENCES

Abbas PJ, & Brown CJ (1991). Electrically evoked auditory brainstem response: Refractory properties and strength-duration functions. Hearing Research, 51(1), 139–147. 10.1016/0378-5955(91)90012-x [PubMed: 2013540]

Abbas PJ, & Brown CJ (2015). Assessment of responses to cochlear implant stimulation at different levels of the auditory pathway. Hearing Research, 322, 67–76. 10.1016/j.heares.2014.10.011 [PubMed: 25445817]

Abbas PJ, Miller CA, Matsuoka AJ, & Rubinstein JT (1997). The neurophysiological effects of simulated auditory prosthesis stimulation. Fourth quarterly progress report. NIH contract N01-DC-6–2111.

Abbas PJ, Miller CA, Rubinstein JT, Robinson BK, Mino H, Hu N, Nourski KV, Jeng FC, & Runge Samuelson CL (2003). Neurophysiological effects of simulated auditory prosthesis stimulation. Final report. NIH contract N01-DC-9–2107.

Adel Y, Hilkhuysen G, Noreña A, Cazals Y, Roman S, & Macherey O (2017). Forward masking in cochlear implant users: Electrophysiological and psychophysical data using pulse train maskers. Journal of the Association for Research in Otolaryngology, 18(3), 495–512. 10.1007/s10162-016-0613-5 [PubMed: 28224320]

Adenis V, Gourévitch B, Mamelle E, Recugnat M, Stahl P, Gnansia D, Nguyen Y, & Edeline J-M (2018). ECAP growth function to increasing pulse amplitude or pulse duration demonstrates large inter-animal variability that is reflected in auditory cortex of the guinea pig. PLOS ONE, 13(8), e0201771. 10.1371/journal.pone.0201771 [PubMed: 30071005]

Agterberg MJH, Versnel H, de Groot JCMJ, Smoorenburg GF, Albers FWJ, & Klis SFL (2008). Morphological changes in spiral ganglion cells after intracochlear application of brain-derived neurotrophic factor in deafened guinea pigs. Hearing Research, 244(1-2), 25–34. 10.1016/j.heares.2008.07.004 [PubMed: 18692557]

Alhabib SF, Abdelsamad Y, Yousef M, & Alzhrani F (2021). Performance of cochlear implant recipients fitted with triphasic pulse patterns. European Archives of Oto-Rhino-Laryngology, 278(9), 3211–3216. 10.1007/s00405-020-06382-0 [PubMed: 32979117]

Avissar M, Wittig JH, Saunders JC, & Parsons TD (2013). Refractoriness enhances temporal coding by auditory nerve fibers. Journal of Neuroscience, 33(18), 7681–7690. 10.1523/jneurosci.3405-12.2013 [PubMed: 23637161]

Bachmaier R, Encke J, Obando-Leitón M, Hemmert W, & Bai S (2019). Comparison of multi-compartment cable models of human auditory nerve fibers. Frontiers in Neuroscience, 13, 1173. 10.3389/fnins.2019.01173 [PubMed: 31749676]

Bahmer A, & Baumann U (2013). Effects of electrical pulse polarity shape on intra cochlear neural responses in humans: Triphasic pulses with cathodic second phase. Hearing Research, 306, 123–130. 10.1016/j.heares.2013.10.001 [PubMed: 24161948]

Bahmer A, & Baumann U (2016). The underlying mechanism of preventing facial nerve stimulation by triphasic pulse stimulation in cochlear implant users assessed with objective measure. Otology & Neurotology, 37(9), 1231–1237. 10.1097/mao.0000000000001156 [PubMed: 27636387]

Battmer RD, Dillier N, Lai WK, Weber BP, Brown C, Gantz BJ, Roland JT, Cohen NJ, Shapiro W, Pesch J, Killian MJ, & Lenarz T (2004). Evaluation of the Neural Response Telemetry (NRT) capabilities of the Nucleus Research Platform 8: initial results from the NRT trial. International Journal of Audiology, 43, S10–S15. [PubMed: 15732376]

Birman CS, Powell HRF, Gibson WPR, & Elliott EJ (2016). Cochlear implant outcomes in cochlea nerve aplasia and hypoplasia. Otology & Neurotology, 37(5), 438–445. 10.1097/mao.0000000000000997 [PubMed: 27050647]

Bittencourt AG, Torre AAGD, Bento RF, Tsuji RK, & Brito R de. (2012). Prelingual deafness: Benefits from cochlear implants versus conventional hearing aids. International Archives of Otorhinolaryngology, 16(3), 387–390. 10.7162/S1809-97772012000300014 [PubMed: 25991962]

Botros A, & Psarros C (2010). Neural response telemetry reconsidered: II. the influence of neural population on the ECAP recovery function and refractoriness. Ear and Hearing, 31(3), 380–391. 10.1097/aud.0b013e3181cb41aa [PubMed: 20090532]

Boulet J, & Bruce IC (2017). Predictions of the contribution of HCN half-maximal activation potential heterogeneity to variability in intrinsic adaptation of spiral ganglion neurons. Journal of the Association for Research in Otolaryngology, 18(2), 301–322. 10.1007/s10162-016-0605-5 [PubMed: 27942887]

Boulet J, White M, & Bruce IC (2016). Temporal considerations for stimulating spiral ganglion neurons with cochlear implants. Journal of the Association for Research in Otolaryngology, 17(1), 1–17. 10.1007/s10162-015-0545-5 [PubMed: 26501873]

Braun K, Walker K, Sürth W, Löwenheim H, & Tropitzsch A (2019). Triphasic pulses in cochlear implant patients with facial nerve stimulation. Otology & Neurotology, 40(10), 1268–1277. 10.1097/mao.0000000000002398 [PubMed: 31469792]

Brochier T, Guérit F, Deeks JM, Garcia C, Bance M, & Carlyon RP (2021a). Evaluating and comparing behavioural and electrophysiological estimates of neural health in cochlear implant users. Journal of the Association for Research in Otolaryngology, 22(1), 67–80. 10.1007/s10162-020-00773-0 [PubMed: 33150541]

Brochier T, McKay CM, & Carlyon RP (2021b). Interpreting the effect of stimulus parameters on the electrically evoked compound action potential and on neural health estimates. Journal of the Association for Research in Otolaryngology, 22(1), 81–94. 10.1007/s10162-020-00774-z [PubMed: 33108575]

Bromm B, & Frankenhaeuser B (1968). Numerical calculation of the response in the myelinated nerve to short symmetrical double pulses. Pflüger's Archiv Für Die Gesamte Physiologie Des Menschen Und Der Tier, 299(4), 357–363.

Brown CJ, Abbas PJ, Etler CP, O'Brien S, & Oleson JJ (2010). Effects of long-term use of a cochlear implant on the electrically evoked compound action potential. Journal of the American Academy of Audiology, 21(01), 005–015. 10.3766/jaaa.21.1.2

Brown CJ, Abbas PJ, & Gantz B (1990). Electrically evoked whole-nerve action potentials: Data from human cochlear implant users. The Journal of the Acoustical Society of America, 88(3), 1385–1391. 10.1121/1.399716 [PubMed: 2229673]

Bruce IC, White MW, Irlicht LS, O'Leary SJ, Dynes S, Javel E, & Clark GM (1999a). A stochastic model of the electrically stimulated auditory nerve: Single-pulse response. IEEE Transactions on Biomedical Engineering, 46(6), 617–629. 10.1109/10.764938 [PubMed: 10356868]

Bruce IC, Irlicht LS, White MW, O'Leary SJ, Dynes S, Javel E, & Clark GM (1999b). A stochastic model of the electrically stimulated auditory nerve: Pulse-train response. IEEE Transactions on Biomedical Engineering, 46(6), 630–637. 10.1109/10.764939 [PubMed: 10356869]

Bruce IC, White MW, Irlicht LS, O'Leary SJ, & Clark GM (1999c). The effects of stochastic neural activity in a model predicting intensity perception with cochlear implants: Low-rate stimulation. IEEE Transactions on Biomedical Engineering, 46(12), 1393–1404. 10.1109/10.804567 [PubMed: 10612897]

Brummer SB, & Turner MJ (1975). Electrical stimulation of the nervous system: The principle of safe charge injection with noble metal electrodes. Bioelectrochemistry and Bioenergetics, 2(1), 13–25. 10.1016/0302-4598(75)80002-x

Cafarelli Dees D, Dillier N, Lai WK, von Wallenberg E, van Dijk B, Akdas F, Aksit M, Batman C, Beynon A, Burdo S, Chanal JM, Collet L, Conway M, Coudert C, Craddock L, Cullington H, Deggouj N, Fraysse B, Grabel S, & Kiefer J (2005). Normative findings of electrically evoked compound action potential measurements using the neural response telemetry of the nucleus CI24M cochlear implant system. Audiology and Neurotology, 10(2), 105–116. 10.1159/000083366 [PubMed: 15650302]

Cartee LA, Miller CA, & van den Honert C (2006). Spiral ganglion cell site of excitation I: Comparison of scala tympani and intrameatal electrode responses. Hearing Research, 215(1-2), 10–21. 10.1016/j.heares.2006.02.012 [PubMed: 16624511]

Cartee LA, van den Honert C, Finley CC, & Miller RL (2000). Evaluation of a model of the cochlear neural membrane. I. Physiological measurement of membrane characteristics in response to intrameatal electrical stimulation. Hearing Research, 146(1-2), 143–152. 10.1016/s0378-5955(00)00109-x [PubMed: 10913891]

Chen JX, Nourmahnad A, O'Malley J, Reinshagen K, Nadol JB, & Quesnel AM (2020). Otopathology in CHARGE syndrome. Laryngoscope Investigative Otolaryngology, 5(1), 157–162. 10.1002/lio2.347 [PubMed: 32128443]

Clague H, Theunissen F, & Miller JP (1997). Effects of adaptation on neural coding by primary sensory interneurons in the cricket cercal system. Journal of Neurophysiology, 77(1), 207–220. 10.1152/jn.1997.77.1.207 [PubMed: 9120562]

Clay KMS, & Brown CJ (2007). Adaptation of the electrically evoked compound action potential (ECAP) recorded from nucleus CI24 cochlear implant users. Ear and Hearing, 28(6), 850–861. 10.1097/aud.0b013e318157671f [PubMed: 17982371]

Cohen LT (2009). Practical model description of peripheral neural excitation in cochlear implant recipients: 5. Refractory recovery and facilitation. Hearing Research, 248(1-2), 1–14. 10.1016/j.heares.2008.11.007 [PubMed: 19110048]

Cohen LT, Richardson LM, Saunders E, & Cowan RSC (2003). Spatial spread of neural excitation in cochlear implant recipients: Comparison of improved ECAP method and psychophysical forward masking. Hearing Research, 179(1-2), 72–87. 10.1016/s0378-5955(03)00096-0 [PubMed: 12742240]

Colombo J, & Parkins CW (1987). A model of electrical excitation of the mammalian auditory-nerve neuron. Hearing Research, 31(3), 287–311. 10.1016/0378-5955(87)90197-3 [PubMed: 3325482]

da Costa Monsanto R, Knoll RM, de Oliveira Penido N, Song G, Santos F, Paparella MM, & Cureoglu S (2022). Otopathologic abnormalities in CHARGE Syndrome. Otolaryngology--Head and Neck Surgery, 166(2), 363–372. 10.1177/01945998211008911 [PubMed: 33874787]

Delgutte B (1980). Representation of speech-like sounds in the discharge patterns of auditory-nerve fibers. The Journal of the Acoustical Society of America, 68(3), 843–857. 10.1121/1.384824 [PubMed: 7419820]

Delgutte B (1997). Auditory neural processing of speech. In Hardcastle WJ & Laver J (Eds.), The Handbook of Phonetic Science. (pp. 507–538). Oxford: Blackwell.

Delgutte B, & Kiang NYS (1984). Speech coding in the auditory nerve: IV. Sounds with consonant-like dynamic characteristics. The Journal of the Acoustical Society of America, 75(3), 897–907. 10.1121/1.390599 [PubMed: 6707319]

Dhuldhoya AN (2013). Characterization of temporal interactions in the auditory nerve of adult and pediatric cochlear implant users [Doctoral Dissertation].

Dynes SBC (1996). Discharge characteristics of auditory nerve fibers for pulsatile electrical stimuli [Doctoral Dissertation].

Dynes SBC, & Delgutte B (1992). Phase-locking of auditory-nerve discharges to sinusoidal electric stimulation of the cochlea. Hearing Research, 58(1), 79–90. 10.1016/0378-5955(92)90011-b [PubMed: 1559909]

Epping WJM (1990). Influence of adaptation on neural sensitivity to temporal characteristics of sound in the dorsal medullary nucleus and torus semicircularis of the grassfrog. Hearing Research, 45(1-2), 1–13. 10.1016/0378-5955(90)90178-r [PubMed: 2345109]

Felix H, Johnsson LG, Gleeson MJ, de Fraissinette A, & Conen V (1992). Morphometric Analysis of the Cochlear Nerve in Man. Acta Oto-Laryngologica, 112(2), 284–287. 10.1080/00016489.1992.11665419 [PubMed: 1604993]

Frijns JHM, de Snoo SL, & Schoonhoven R (1995). Potential distributions and neural excitation patterns in a rotationally symmetric model of the electrically stimulated cochlea. Hearing Research, 87(1-2), 170–186. 10.1016/0378-5955(95)00090-q [PubMed: 8567435]

Fulmer SL, Runge CL, Jensen JW, & Friedland DR (2010). Rate of neural recovery in implanted children with auditory neuropathy spectrum disorder. Otolaryngology--Head and Neck Surgery, 144(2), 274–279. 10.1177/0194599810391603 [PubMed: 21493430]

Galvin KL, Mok M, & Dowell RC (2007). Perceptual benefit and functional outcomes for children using sequential bilateral cochlear implants. Ear and Hearing, 28(4), 470–482. 10.1097/aud.0b013e31806dc194 [PubMed: 17609610]

Goldwyn JH, Rubinstein JT, & Shea-Brown E (2012). A point process framework for modeling electrical stimulation of the auditory nerve. Journal of Neurophysiology, 108(5), 1430–1452. 10.1152/jn.00095.2012 [PubMed: 22673331]

Goutman JD, & Glowatzki E (2007). Time course and calcium dependence of transmitter release at a single ribbon synapse. Proceedings of the National Academy of Sciences, 104(41), 16341–16346. 10.1073/pnas.0705756104

Haenggeli A, Zhang JS, Fischer MW, Pelizzone M, & Rouiller EM (1998). Electrically evoked compound action potential (ECAP) of the cochlear nerve in response to pulsatile electrical stimulation of the cochlea in the rat: Effects of stimulation at high rates. International Journal of Audiology, 37(6), 353–371. 10.3109/00206099809072989

Hall RD (1990). Estimation of surviving spiral ganglion cells in the deaf rat using the electrically evoked auditory brainstem response. Hearing Research, 49(1-3), 155–168. 10.1016/0378-5955(90)90102-u [PubMed: 2292495]

Han JJ, Suh M-W, Park MK, Koo J-W, Lee JH, & Oh SH (2019). A predictive model for cochlear implant outcome in children with cochlear nerve deficiency. Scientific Reports, 9(1). 10.1038/s41598-018-37014-7

Hartmann R, Topp G, & Klinke R (1984). Discharge patterns of cat primary auditory fibers with electrical stimulation of the cochlea. Hearing Research, 13(1), 47–62. 10.1016/0378-5955(84)90094-7 [PubMed: 6546751]

Hay-McCutcheon MJ, Brown CJ, & Abbas PJ (2005). An analysis of the impact of auditory-nerve adaptation on behavioral measures of temporal integration in cochlear implant recipients. The Journal of the Acoustical Society of America, 118(4), 2444–2457. 10.1121/1.2035593 [PubMed: 16266166]

He S, Abbas PJ, Doyle DV, McFayden TC, & Mulherin S (2016). Temporal response properties of the auditory nerve in implanted children with auditory neuropathy spectrum disorder and implanted children with sensorineural hearing loss. Ear and Hearing, 37(4), 397–411. 10.1097/aud.0000000000000254 [PubMed: 26655913]

He S, Shahsavarani BS, McFayden TC, Wang H, Gill KE, Xu L, Chao X, Luo J, Wang R, & He N (2018). Responsiveness of the electrically stimulated cochlear nerve in children with cochlear nerve deficiency. Ear and Hearing, 39(2), 238–250. 10.1097/aud.0000000000000467 [PubMed: 28678078]

He S, Skidmore J, Conroy S, Riggs WJ, Carter BL, & Xie R (2022a). Neural adaptation of the electrically stimulated auditory nerve is not affected by advanced age in postlingually deafened, middle-aged, and elderly adult cochlear implant users. Ear and Hearing, 43(4), 1228–1244. 10.1097/aud.0000000000001184 [PubMed: 34999595]

He S, Skidmore J, & Carter BL (2022b). Characteristics of the adaptation recovery function of the auditory nerve and its association with advanced age in postlingually deafened adult cochlear implant users. Ear and Hearing, 43(5), 1472–1486. 10.1097/aud.0000000000001198 [PubMed: 35139051]

He S, Skidmore J, Chatterjee M, Carter BL, Lemeshow S, & Sun S (2022c). Postlingually deafened adult cochlear implant users with prolonged recovery from neural adaptation at the level of the auditory nerve tend to have poorer speech perception performance. Ear and Hearing, Publish Ahead of Print. 10.1097/aud.0000000000001244

He S, Xu L, Skidmore J, Chao X, Riggs WJ, Wang R, Vaughan C, Luo J, Shannon M, & Warner C (2020a). Effect of increasing pulse phase duration on neural responsiveness of the electrically stimulated cochlear nerve. Ear and Hearing, 41(6), 1606–1618. 10.1097/aud.0000000000000876 [PubMed: 33136636]

He S, Xu L, Skidmore J, Chao X, Jeng F-C, Wang R, Luo J, & Wang H (2020b). The effect of interphase gap on neural response of the electrically stimulated cochlear nerve in children with cochlear nerve deficiency and children with normal-sized cochlear nerves. Ear and Hearing, 41(4), 918–934. 10.1097/aud.0000000000000815 [PubMed: 31688319]

Heffer LF, Sly DJ, Fallon JB, White MW, Shepherd RK, & O'Leary SJ (2010). Examining the auditory nerve fiber response to high rate cochlear implant stimulation: Chronic sensorineural hearing loss and facilitation. Journal of Neurophysiology, 104(6), 3124–3135. 10.1152/jn.00500.2010 [PubMed: 20926607]

Herrmann DP, Kretzer KVA, Pieper SH, & Bahmer A (2021). Effects of electrical pulse polarity shape on intra cochlear neural responses in humans: Triphasic pulses with anodic and cathodic second phase. Hearing Research, 412, 108375. 10.1016/j.heares.2021.108375 [PubMed: 34749281]

Heshmat A, Sajedi S, Johnson Chacko L, Fischer N, Schrott-Fischer A, & Rattay F (2020). Dendritic degeneration of human auditory nerve fibers and its impact on the spiking pattern under regular conditions and during cochlear implant stimulation. Frontiers in Neuroscience, 14, 599868. 10.3389/fnins.2020.599868 [PubMed: 33328872]

Hey M, Müller-Deile J, Hessel H, & Killian M (2017). Facilitation and refractoriness of the electrically evoked compound action potential. Hearing Research, 355, 14–22. 10.1016/j.heares.2017.09.001 [PubMed: 28947082]

Horne CDF, Sumner CJ, & Seeber BU (2016). A phenomenological model of the electrically stimulated auditory nerve fiber: Temporal and biphasic response properties. Frontiers in Computational Neuroscience, 10. 10.3389/fncom.2016.00008

Huarte A, Ramos A, Morera C, Garcia-Ibáñez L, Battmer R, Dillier N, Wesarg T, Müller-Deile J, Hey M, Offeciers E, von Wallenberg E, Coudert C, & Killian M (2014). Evaluation of neural response telemetry (NRTTM) with focus on long-term rate adaptation over a wide range of stimulation rates. Cochlear Implants International, 15(3), 136–144. 10.1179/1754762814y.0000000063 [PubMed: 24559068]

Hughes ML (2022). Characterizing polarity sensitivity in cochlear implant recipients: Demographic effects and potential implications for estimating neural health. Journal of the Association for Research in Otolaryngology, 23(2), 301–318. 10.1007/s10162-021-00824-0 [PubMed: 34988867]

Hughes ML, & Abbas PJ (2006). The relation between electrophysiologic channel interaction and electrode pitch ranking in cochlear implant recipients. The Journal of the Acoustical Society of America, 119(3), 1527–1537. 10.1121/1.2163273 [PubMed: 16583898]

Hughes ML, Baudhuin JL, & Goehring JL (2014). The relation between auditory-nerve temporal responses and perceptual rate integration in cochlear implants. Hearing Research, 316, 44–56. 10.1016/j.heares.2014.07.007 [PubMed: 25093283]

Hughes ML, Castioni EE, Goehring JL, & Baudhuin JL (2012). Temporal response properties of the auditory nerve: Data from human cochlear-implant recipients. Hearing Research, 285(1-2), 46–57. 10.1016/j.heares.2012.01.010 [PubMed: 22326590]

Hughes ML, Goehring JL, & Baudhuin JL (2017). Effects of stimulus polarity and artifact reduction method on the electrically evoked compound action potential. Ear and Hearing, 38(3), 332–343. 10.1097/aud.0000000000000392 [PubMed: 28045836]

Hughes ML, & Laurello SA (2017). Effect of stimulus level on the temporal response properties of the auditory nerve in cochlear implants. Hearing Research, 351, 116–129. 10.1016/j.heares.2017.06.004 [PubMed: 28633960]

Hu N, Miller CA, Abbas PJ, Robinson BK, & Woo J (2010). Changes in auditory nerve responses across the duration of sinusoidally amplitude-modulated electric pulse-train stimuli. Journal of the Association for Research in Otolaryngology, 11(4), 641–656. 10.1007/s10162-010-0225-4 [PubMed: 20632064]

Imennov NS, & Rubinstein JT (2009). Stochastic population model for electrical stimulation of the auditory nerve. IEEE Transactions on Biomedical Engineering, 56(10), 2493–2501. 10.1109/tbme.2009.2016667 [PubMed: 19304476]

Imsiecke M, Büchner A, Lenarz T, & Nogueira W (2021). Amplitude growth functions of auditory nerve responses to electric pulse stimulation with varied interphase gaps in cochlear implant users with ipsilateral residual hearing. Trends in Hearing, 25, 233121652110141. 10.1177/23312165211014137

Jackler RK, Luxfor WM, & House WF (1987). Congenital malformations of the inner ear: A classification based on embryogenesis. The Laryngoscope, 97(S40), 2–14. 10.1002/lary.5540971301 [PubMed: 3821363]

Jahn KN, & Arenberg JG (2020a). Electrophysiological estimates of the electrode–neuron interface differ between younger and older listeners with cochlear implants. Ear and Hearing, 41(4), 948–960. 10.1097/aud.0000000000000827 [PubMed: 32032228]

Jahn KN, & Arenberg JG (2020b). Identifying cochlear implant channels with relatively poor electrode-neuron interfaces using the electrically evoked compound action potential. Ear and Hearing, 41(4), 961–973. 10.1097/aud.0000000000000844 [PubMed: 31972772]

Jahn KN, DeVries L, & Arenberg JG (2021). Recovery from forward masking in cochlear implant listeners: Effects of age and the electrode-neuron interface. The Journal of the Acoustical Society of America, 149(3), 1633–1643. 10.1121/10.0003623 [PubMed: 33765782]

Javel E (1990). Acoustic and electrical encoding of temporal information. In Miller JM & Spelman FA (Eds.), Cochlear implants. Models of the Electrically Stimulated Ear (pp. 247–295). Springer.

Javel E, Tong YC, Shepherd RK, & Clark GM (1987). Responses of cat auditory nerve fibers to biphasic electrical current pulses. Annals of Otology, Rhinology & Laryngology, 96(1_suppl), 26–30. 10.1177/00034894870960s111 [PubMed: 3813382]

Jeng F-C, Abbas PJ, Hu N, Miller CA, Nourski KV, & Robinson BK (2009). Effects of temporal properties on compound action potentials in response to amplitude-modulated electric pulse trains in guinea pigs. Hearing Research, 247(1), 47–59. 10.1016/j.heares.2008.10.007 [PubMed: 19015019]

Johnson DH (1980). The relationship between spike rate and synchrony in responses of auditory-nerve fibers to single tones. The Journal of the Acoustical Society of America, 68(4), 1115–1122. 10.1121/1.384982 [PubMed: 7419827]

Joshi SN, Dau T, & Epp B (2017). A model of electrically stimulated auditory nerve fiber responses with peripheral and central sites of spike generation. Journal of the Association for Research in Otolaryngology, 18(2), 323–342. 10.1007/s10162-016-0608-2 [PubMed: 28054149]

Jun AI, McGuirt WT, Hinojosa R, Green GE, Fischel-Ghodsian N, & Smith RJH (2000). Temporal bone histopathology in connexin 26-related hearing loss. The Laryngoscope, 110(2), 269–269. 10.1097/00005537-200002010-00016 [PubMed: 10680928]

Karg SA, Lackner C, & Hemmert W (2013). Temporal interaction in electrical hearing elucidates auditory nerve dynamics in humans. Hearing Research, 299, 10–18. 10.1016/j.heares.2013.01.015 [PubMed: 23396273]

Killian MJP, Klis SFL, & Smoorenburg GF (1994). Adaptation in the compound action potential response of the guinea pig VIIIth nerve to electric stimulation. Hearing Research, 81(1-2), 66–82. 10.1016/0378-5955(94)90154-6 [PubMed: 7737931]

Kim BG, Chung HJ, Park JJ, Park S, Kim SH, & Choi JY (2013). Correlation of cochlear nerve size and auditory performance after cochlear implantation in postlingually deaf patients. JAMA Otolaryngology–Head & Neck Surgery, 139(6), 604–609. 10.1001/jamaoto.2013.3195 [PubMed: 23787419]

Kim J-R, Abbas PJ, Brown CJ, Etler CP, O'Brien S, & Kim L-S (2010). The relationship between electrically evoked compound action potential and speech perception. Otology & Neurotology, 31(7), 1041–1048. 10.1097/mao.0b013e3181ec1d92 [PubMed: 20634770]

Kim J-R, Kim L-S, Jeong S-W, Kim J-S, & Chung S-H (2011). Recovery function of electrically evoked compound action potential in implanted children with auditory neuropathy: Preliminary results. Acta Oto-Laryngologica, 131(8), 796–801. 10.3109/00016489.2011.560187 [PubMed: 21466261]

Kirby B, Brown C, Abbas P, Etler C, & O'Brien S (2012). Relationships between electrically evoked potentials and loudness growth in bilateral cochlear implant users. Ear and Hearing, 33(3), 389–398. 10.1097/aud.0b013e318239adb8 [PubMed: 22246138]

Kirk EC, & Gosselin-Ildari AD (2009). Cochlear labyrinth volume and hearing abilities in primates. The Anatomical Record: Advances in Integrative Anatomy and Evolutionary Biology, 292(6), 765–776. 10.1002/ar.20907 [PubMed: 19462443]

Klop WMC, Hartlooper A, Briare JJ, & Frijns JHM (2004). A new method for dealing with the stimulus artefact in electrically evoked compound action potential measurements. Acta Oto-Laryngologica, 124(2), 137–143. 10.1080/00016480310016901 [PubMed: 15072415]

Konerding W, Arenberg JG, Kral A, & Baumhoff P (2022). Late electrically-evoked compound action potentials as markers for acute micro-lesions of spiral ganglion neurons. Hearing Research, 108057. 10.1016/j.heares.2020.108057 [PubMed: 32883545]

Kopsch AC, Rahne T, Plontke SK, & Wagner L (2022). Influence of the spread of electric field on neural excitation in cochlear implant users: Transimpedance and spread of excitation measurements. Hearing Research, 424, 108591. 10.1016/j.heares.2022.108591 [PubMed: 35914395]

Kroon S, Ramekers D, Smeets EM, Hendriksen FGJ, Klis SFL, & Versnel H (2017). Degeneration of auditory nerve fibers in guinea pigs with severe sensorineural hearing loss. Hearing Research, 345, 79–87. 10.1016/j.heares.2017.01.005 [PubMed: 28087418]

Langner F, Arenberg JG, Büchner A, & Nogueira W (2021). Assessing the relationship between neural health measures and speech performance with simultaneous electric stimulation in cochlear implant listeners. PLoS One, 16(12), e0261295. 10.1371/journal.pone.0261295 [PubMed: 34898654]

Lapicque L (1907). Recherches quantitatives sur l'excitation electrique des nerfs traitee comme une polarization. Journal of Physiology-Paris, 9, 620–635.

Leake PA, & Hradek GT (1988). Cochlear pathology of long term neomycin induced deafness in cats. Hearing Research, 33(1), 11–33. 10.1016/0378-5955(88)90018-4 [PubMed: 3372368]

Lee ER, Friedland DR, & Runge CL (2012). Recovery from forward masking in elderly cochlear implant users. Otology & Neurotology, 33(3), 355–363. 10.1097/mao.0b013e318248ede5 [PubMed: 22410729]

Lenarz M, Sönmez H, Joseph G, Büchner A, & Lenarz T (2012). Cochlear implant performance in geriatric patients. The Laryngoscope, 122(6), 1361–1365. 10.1002/lary.23232 [PubMed: 22539093]

Liberman MC, & Oliver ME (1984). Morphometry of intracellularly labeled neurons of the auditory nerve: Correlations with functional properties. The Journal of Comparative Neurology, 223(2), 163–176. 10.1002/cne.902230203 [PubMed: 6200517]

Litvak L, Delgutte B, & Eddington D (2001). Auditory nerve fiber responses to electric stimulation: Modulated and unmodulated pulse trains. The Journal of the Acoustical Society of America, 110(1), 368–379. 10.1121/1.1375140 [PubMed: 11508961]

Litvak LM, Delgutte B, & Eddington DK (2003a). Improved temporal coding of sinusoids in electric stimulation of the auditory nerve using desynchronizing pulse trains. The Journal of the Acoustical Society of America, 114(4), 2079–2098. 10.1121/1.1612493 [PubMed: 14587607]

Litvak LM, Smith ZM, Delgutte B, & Eddington DK (2003b). Desynchronization of electrically evoked auditory-nerve activity by high-frequency pulse trains of long duration. The Journal of the Acoustical Society of America, 114(4), 2066–2078. 10.1121/1.1612492 [PubMed: 14587606]

Liu W, Boström M, Kinnefors A, Linthicum F, & Rask-Andersen H (2012). Expression of myelin basic protein in the human auditory nerve—An immunohistochemical and comparative study. Auris Nasus Larynx, 39(1), 18–24. 10.1016/j.anl.2011.04.007 [PubMed: 21601398]

Liu Z, Cakir A, & Noble JH (2020). Auditory nerve fiber health estimation using patient specific cochlear implant stimulation models. In International Workshop on Simulation and Synthesis in Medical Imaging (pp. 184–194). Springer.

Loeb GE, White MW, & Jenkins WM (1983). Biophysical considerations in electrical stimulation of the auditory nervous system. Annals of the New York Academy of Sciences, 405(1), 123–136. 10.1111/j.1749-6632.1983.tb31625.x [PubMed: 6575638]

Luo J, Xu L, Chao X, Wang R, Pellittieri A, Bai X, Fan Z, Wang H, & He S (2020). The effects of GJB2 or SLC26A4 gene mutations on neural response of the electrically stimulated auditory nerve in children. Ear and Hearing, 41(1), 194–207. 10.1097/aud.0000000000000744 [PubMed: 31124793]

Macherey O, Carlyon RP, van Wieringen A, Deeks JM, & Wouters J (2008). Higher sensitivity of human auditory nerve fibers to positive electrical currents. Journal of the Association for Research in Otolaryngology, 9(2), 241–251. 10.1007/s10162-008-0112-4 [PubMed: 18288537]

Macherey O, & Cazals Y (2016). Effects of pulse shape and polarity on sensitivity to cochlear implant stimulation: A chronic study in guinea pigs. In Physiology, Psychoacoustics and Cognition in Normal and Impaired Hearing (pp. 133–142). Springer, Cham.

Macherey O, van Wieringen A, Carlyon RP, Deeks JM, & Wouters J (2006). Asymmetric pulses in cochlear implants: Effects of pulse shape, polarity, and rate. Journal of the Association for Research in Otolaryngology, 7(3), 253–266. 10.1007/s10162-006-0040-0 [PubMed: 16715356]

Makary CA, Shin J, Kujawa SG, Liberman MC, & Merchant SN (2011). Age-Related primary cochlear neuronal degeneration in human temporal bones. Journal of the Association for Research in Otolaryngology, 12(6), 711–717. 10.1007/s10162-011-0283-2 [PubMed: 21748533]

Matsuoka AJ, Abbas PJ, Rubinstein JT, & Miller CA (2000a). The neuronal response to electrical constant-amplitude pulse train stimulation: Evoked compound action potential recordings. Hearing Research, 149(1-2), 115–128. 10.1016/s0378-5955(00)00172-6 [PubMed: 11033251]

Matsuoka AJ, Abbas PJ, Rubinstein JT, & Miller CA (2000b). The neuronal response to electrical constant-amplitude pulse train stimulation: Additive Gaussian noise. Hearing Research, 149(1-2), 129–137. 10.1016/s0378-5955(00)00173-8 [PubMed: 11033252]

McKay CM, Chandan K, Akhoun I, Siciliano C, & Kluk K (2013). Can ECAP measures be used for totally objective programming of cochlear implants? Journal of the Association for Research in Otolaryngology, 14(6), 879–890. 10.1007/s10162-013-0417-9 [PubMed: 24048907]

Merrill DR, Bikson M, & Jefferys JGR (2005). Electrical stimulation of excitable tissue: Design of efficacious and safe protocols. Journal of Neuroscience Methods, 141(2), 171–198. 10.1016/j.jneumeth.2004.10.020 [PubMed: 15661300]

Meyer K, Rouiller EM, & Loquet G (2007). Direct comparison between properties of adaptation of the auditory nerve and the ventral cochlear nucleus in response to repetitive clicks. Hearing Research, 228(1-2), 144–155. 10.1016/j.heares.2007.02.002 [PubMed: 17391881]

Middlebrooks JC (2004). Effects of cochlear-implant pulse rate and inter-channel timing on channel interactions and thresholds. The Journal of the Acoustical Society of America, 116(1), 452–468. 10.1121/1.1760795 [PubMed: 15296005]

Miller AL, Smith DW, & Pfingst BE (1999b). Across-species comparisons of psychophysical detection thresholds for electrical stimulation of the cochlea: I. Sinusoidal stimuli. Hearing Research, 134(1-2), 89–104. 10.1016/s0378-5955(99)00072-6 [PubMed: 10452379]

Miller CA, Abbas PJ, Hay-McCutcheon MJ, Robinson BK, Nourski KV, & Jeng F-C (2004). Intracochlear and extracochlear ECAPs suggest antidromic action potentials. Hearing Research, 198(1-2), 75–86. 10.1016/j.heares.2004.07.005 [PubMed: 15567605]

Miller CA, Abbas PJ, Nourski KV, Hu N, & Robinson BK (2003). Electrode configuration influences action potential initiation site and ensemble stochastic response properties. Hearing Research, 175(1-2), 200–214. 10.1016/s0378-5955(02)00739-6 [PubMed: 12527139]

Miller CA, Abbas PJ, & Robinson BK (2001a). Response properties of the refractory auditory nerve fiber. Journal of the Association for Research in Otolaryngology, 2(3), 216–232. 10.1007/s101620010083 [PubMed: 11669395]

Miller CA, Abbas PJ, Robinson BK, Nourski KV, Zhang F, & Jeng F-C (2009). Auditory nerve fiber responses to combined acoustic and electric stimulation. Journal of the Association for Research in Otolaryngology, 10(3), 425–445. 10.1007/s10162-008-0154-7 [PubMed: 19205803]

Miller CA, Abbas PJ, Robinson BK, Rubinstein JT, & Matsuoka AJ (1999a). Electrically evoked single-fiber action potentials from cat: Responses to monopolar, monophasic stimulation. Hearing Research, 130(1-2), 197–218. 10.1016/s0378-5955(99)00012-x [PubMed: 10320109]

Miller CA, Abbas PJ, Rubinstein JT, Robinson BK, Matsuoka AJ, & Woodworth G (1998). Electrically evoked compound action potentials of guinea pig and cat: Responses to monopolar, monophasic stimulation. Hearing Research, 119(1-2), 142–154. 10.1016/s0378-5955(98)00046-x [PubMed: 9641327]

Miller CA, Hu N, Zhang F, Robinson BK, & Abbas PJ (2008). Changes across time in the temporal responses of auditory nerve fibers stimulated by electric pulse trains. Journal of the Association for Research in Otolaryngology, 9(1), 122–137. 10.1007/s10162-007-0108-5 [PubMed: 18204987]

Miller CA, Robinson BK, Rubinstein JT, Abbas PJ, & Runge-Samuelson CL (2001b). Auditory nerve responses to monophasic and biphasic electric stimuli. Hearing Research, 151(1-2), 79–94. 10.1016/s0300-2977(00)00082-6 [PubMed: 11124454]

Miller CA, Woodruff KE, & Pfingst BE (1995). Functional responses from guinea pigs with cochlear implants. I. Electrophysiological and psychophysical measures. Hearing Research, 92(1-2), 85–99. 10.1016/0378-5955(95)00204-9 [PubMed: 8647749]

Miller CA, Woo J, Abbas PJ, Hu N, & Robinson BK (2011). Neural masking by sub-threshold electric stimuli: Animal and computer model results. Journal of the Association for Research in Otolaryngology, 12(2), 219–232. 10.1007/s10162-010-0249-9 [PubMed: 21080206]

Miyagawa M, Nishio S-Y, & Usami S-I (2016). A comprehensive study on the etiology of patients receiving cochlear implantation with special emphasis on genetic epidemiology. Otology & Neurotology, 37(2), e126–e134. 10.1097/mao.0000000000000936 [PubMed: 26756145]

Moberly AC, Bates C, Harris MS, & Pisoni DB (2016). The enigma of poor performance by adults with cochlear implants. Otology & Neurotology, 37(10), 1522–1528. 10.1097/MAO.0000000000001211 [PubMed: 27631833]

Morsnowski A, Charasse B, Collet L, Killian M, & Müller-Deile J (2006). Measuring the refractoriness of the electrically stimulated auditory nerve. Audiology and Neurotology, 11(6), 389–402. 10.1159/000095966 [PubMed: 17008774]

Motz H, & Rattay F (1986). A study of the application of the Hodgkin-Huxley and the Frankenhaeuser-Huxley model for electrostimulation of the acoustic nerve. Neuroscience, 18(3), 699–712. 10.1016/0306-4522(86)90064-3 [PubMed: 3748378]

Moxon EC (1971). Neural and mechanical responses to electric stimulation of the cat's inner ear [Doctoral Dissertation].

Mussoi BSS, & Brown CJ (2019). Age-Related changes in temporal resolution revisited. Ear and Hearing, 40(6), 1328–1344. 10.1097/aud.0000000000000732 [PubMed: 31033701]

Mussoi BSS, & Brown CJ (2020). The effect of aging on the electrically evoked compound action potential. Otology & Neurotology, 41(7), e804–e811. 10.1097/mao.0000000000002688 [PubMed: 32501933]

Nadol JB (1988). Comparative anatomy of the cochlea and auditory nerve in mammals. Hearing Research, 34(3), 253–266. 10.1016/0378-5955(88)90006-8 [PubMed: 3049492]

Nadol JB, Adams JC, & O'Malley JT (2012). Temporal bone histopathology in a case of sensorineural hearing loss caused by superficial siderosis of the central nervous system and treated by cochlear implantation. Otology & Neurotology, 32(5), 748–755. 10.1097/mao.0b013e31820e7195

Nadol JB, Young Y-S, & Glynn RJ (1989). Survival of spiral ganglion cells in profound sensorineural hearing loss: Implications for cochlear implantation. Annals of Otology, Rhinology & Laryngology, 98(6), 411–416. 10.1177/000348948909800602 [PubMed: 2729822]

Navntoft CA, Landsberger DM, Barkat TR, & Marozeau J (2021). The perception of ramped pulse shapes in cochlear implant users. Trends in Hearing, 25, 233121652110611. 10.1177/23312165211061116

Navntoft CA, Marozeau J, & Barkat TR (2020). Ramped pulse shapes are more efficient for cochlear implant stimulation in an animal model. Scientific Reports, 10(1), 1–17. 10.1038/s41598-020-60181-5 [PubMed: 31913322]

Negm MH, & Bruce IC (2014). The effects of HCN and KLT ion channels on adaptation and refractoriness in a stochastic auditory nerve model. IEEE Transactions on Biomedical Engineering, 61(11), 2749–2759. 10.1109/tbme.2014.2327055 [PubMed: 24893366]

Nelson EG, & Hinojosa R (2001). Aplasia of the cochlear nerve: A temporal bone study. Otology & Neurotology, 22(6), 790–795. 10.1097/00129492-200111000-00013 [PubMed: 11698797]

Nourski KV, Abbas PJ, Miller CA, Robinson BK, & Jeng F-C (2007). Acoustic–electric interactions in the guinea pig auditory nerve: Simultaneous and forward masking of the electrically evoked compound action potential. Hearing Research, 232(1-2), 87–103. 10.1016/j.heares.2007.07.001 [PubMed: 17723284]

Ota CY, & Kimura RS (1980). Ultrastructural study of the human spiral ganglion. Acta Oto-Laryngologica, 89(1-2), 53–62. 10.3109/00016488009127108 [PubMed: 7405577]

Parkins CW (1989). Temporal response patterns of auditory nerve fibers to electrical stimulation in deafened squirrel monkeys. Hearing Research, 41(2-3), 137–168. 10.1016/0378-5955(89)90007-5 [PubMed: 2808146]

Parkins CW, & Colombo J (1987). Auditory-nerve single-neuron thresholds to electrical stimulation from scala tympani electrodes. Hearing Research, 31(3), 267–285. 10.1016/0378-5955(87)90196-1 [PubMed: 3436853]

Pesch J, Lai WK,Killian M, Lenarz T, & Battmer RD (2005, July 30 – August 4). Characteristicsof NRT™ recovery functions for different stimulation parameters [Posterpresentation]. Conference on Implantable Auditory Prostheses, Pacific Grove,CA.

Pfingst BE, Colesa DJ, Swiderski DL, Hughes AP, Strahl SB, Sinan M, & Raphael Y (2017). Neurotrophin gene therapy in deafened ears with cochlear implants: Long-term effects on nerve survival and functional measures. Journal of the Association for Research in Otolaryngology, 18(6), 731–750. 10.1007/s10162-017-0633-9 [PubMed: 28776202]

Pfingst BE, Hughes AP, Colesa DJ, Watts MM, Strahl SB, & Raphael Y (2015a). Insertion trauma and recovery of function after cochlear implantation: Evidence from objective functional measures. Hearing Research, 330, 98–105. 10.1016/j.heares.2015.07.010 [PubMed: 26209185]

Pfingst BE, Zhou N, Colesa DJ, Watts MM, Strahl SB, Garadat SN, Schvartz-Leyzac KC, Budenz CL, Raphael Y, & Zwolan TA (2015b). Importance of cochlear health for implant function. Hearing Research, 322, 77–88. 10.1016/j.heares.2014.09.009 [PubMed: 25261772]

Prado-Guitierrez P, Fewster LM, Heasman JM, McKay CM, & Shepherd RK (2006). Effect of interphase gap and pulse duration on electrically evoked potentials is correlated with auditory

nerve survival. Hearing Research, 215(1-2), 47–55. 10.1016/j.heares.2006.03.006 [PubMed: 16644157]

Ramekers D, Benav H, Klis SFL, & Versnel H (2022). Changes in the electrically evoked compound action potential over time after implantation and subsequent deafening in guinea pigs. Journal of the Association for Research in Otolaryngology. 10.1007/s10162-022-00864-0

Ramekers D, Klis SFL, & Versnel H (2020). Simultaneous rather than retrograde spiral ganglion cell degeneration following ototoxically induced hair cell loss in the guinea pig cochlea. Hearing Research, 390, 107928. 10.1016/j.heares.2020.107928 [PubMed: 32143110]

Ramekers D, Versnel H, Strahl SB, Klis SFL, & Grolman W (2015a). Recovery characteristics of the electrically stimulated auditory nerve in deafened guinea pigs: Relation to neuronal status. Hearing Research, 321, 12–24. 10.1016/j.heares.2015.01.001 [PubMed: 25582354]

Ramekers D, Versnel H, Strahl SB, Klis SFL, & Grolman W (2015b). Temporary neurotrophin treatment prevents deafness-induced auditory nerve degeneration and preserves function. Journal of Neuroscience, 35(36), 12331–12345. 10.1523/jneurosci.0096-15.2015 [PubMed: 26354903]

Ramekers D, Versnel H, Strahl SB, Smeets EM, Klis SFL, & Grolman W (2014). Auditory-Nerve responses to varied inter-phase gap and phase duration of the electric pulse stimulus as predictors for neuronal degeneration. Journal of the Association for Research in Otolaryngology, 15(2), 187–202. 10.1007/s10162-013-0440-x [PubMed: 24469861]

Rasmussen KMB, West NC, Bille M, Sandvej MG, & Cayé-Thomasen P (2022). Cochlear implantation improves both speech perception and patient-reported outcomes: A prospective follow-up study of treatment benefits among adult cochlear implant recipients. Journal of Clinical Medicine, 11(8), 2257. 10.3390/jcm11082257 [PubMed: 35456353]

Rattay F (1990). Electrical nerve stimulation: Theory, experiments and applications. Springer-Verlag.

Rattay F, Lutter P, & Felix H (2001a). A model of the electrically excited human cochlear neuron. I. Contribution of neural substructures to the generation and propagation of spikes. Hearing Research, 153(1-2), 43–63. 10.1016/s0378-5955(00)00256-2 [PubMed: 11223296]

Rattay F, Leao RN, & Felix H (2001b). A model of the electrically excited human cochlear neuron. II. Influence of the three-dimensional cochlear structure on neural excitability. Hearing Research, 153(1-2), 64–79. 10.1016/s0378-5955(00)00257-4 [PubMed: 11223297]

Rattay F, Potrusil T, Wenger C, Wise AK, Glueckert R, & Schrott-Fischer A (2013). Impact of morphometry, myelinization and synaptic current strength on spike conduction in human and cat spiral ganglion neurons. PloS One, 8(11), e79256. 10.1371/journal.pone.0079256 [PubMed: 24260179]

Resnick JM, O'Brien GE, & Rubinstein JT (2018). Simulated auditory nerve axon demyelination alters sensitivity and response timing to extracellular stimulation. Hearing Research, 361, 121–137. 10.1016/j.heares.2018.01.014 [PubMed: 29496363]

Riggs WJ, Vaughan C, Skidmore J, Conroy S, Pellittieri A, Carter BL, Stegman CJ, & He S (2021). The sensitivity of the electrically stimulated auditory nerve to amplitude modulation cues declines with advanced age. Ear and Hearing, 42(5), 1358–1372. 10.1097/aud.0000000000001035 [PubMed: 33795616]

Rubinstein JT, Miller CA, Mino H, & Abbas PJ (2001). Analysis of monophasic and biphasic electrical stimulation of nerve. IEEE Transactions on Biomedical Engineering, 48(10), 1065–1070. 10.1109/10.951508 [PubMed: 11585029]

Rumeau C, Frère J, Montaut-Verient B, Lion A, Gauchard G, & Parietti-Winkler C (2014). Quality of life and audiologic performance through the ability to phone of cochlear implant users. European Archives of Oto-Rhino-Laryngology, 272(12), 3685–3692. 10.1007/s00405-014-3448-x [PubMed: 25527411]

Runge-Samuelson CL, Abbas PJ, Rubinstein JT, Miller CA, & Robinson BK (2004). Response of the auditory nerve to sinusoidal electrical stimulation: Effects of high-rate pulse trains. Hearing Research, 194(1-2), 1–13. 10.1016/j.heares.2004.03.020 [PubMed: 15276671]

Saeedi A, Englert L, & Hemmert W (2021). eABR THR Estimation Using High-Rate Multi-Pulse Stimulation in Cochlear Implant Users. Frontiers in Neuroscience, 15. 10.3389/fnins.2021.705189

Schvartz-Leyzac KC, Colesa DJ, Buswinka CJ, Swiderski DL, Raphael Y, & Pfingst BE (2019). Changes over time in the electrically evoked compound action potential (ECAP) interphase gap (IPG) effect following cochlear implantation in Guinea pigs. Hearing Research, 383, 107809. 10.1016/j.heares.2019.107809 [PubMed: 31630082]

Schvartz-Leyzac KC, & Pfingst BE (2016). Across-site patterns of electrically evoked compound action potential amplitude-growth functions in multichannel cochlear implant recipients and the effects of the interphase gap. Hearing Research, 341, 50–65. 10.1016/j.heares.2016.08.002 [PubMed: 27521841]

Schvartz-Leyzac KC, & Pfingst BE (2018). Assessing the relationship between the electrically evoked compound action potential and speech recognition abilities in bilateral cochlear implant recipients. Ear and Hearing, 39(2), 344–358. 10.1097/aud.0000000000000490 [PubMed: 28885234]

Shader MJ, Gordon-Salant S, & Goupell MJ (2020). Impact of aging and the electrode-to-neural interface on temporal processing ability in cochlear-implant users: Gap detection thresholds. Trends in Hearing, 24, 233121652095656. 10.1177/2331216520956560

Shearer AE, Eppsteiner RW, Frees K, Tejani V, Sloan-Heggen CM, Brown C, Abbas P, Dunn C, Hansen MR, Gantz BJ, & Smith RJH (2017). Genetic variants in the peripheral auditory system significantly affect adult cochlear implant performance. Hearing Research, 348, 138–142. 10.1016/j.heares.2017.02.008 [PubMed: 28213135]

Shepherd RK, Hardie NA, & Baxi JH (2001). Electrical stimulation of the auditory nerve: Single neuron strength-duration functions in deafened animals. Annals of Biomedical Engineering, 29(3), 195–201. 10.1114/1.1355276 [PubMed: 11310781]

Shepherd RK, & Javel E (1997). Electrical stimulation of the auditory nerve. I. Correlation of physiological responses with cochlear status. Hearing Research, 108(1-2), 112–144. 10.1016/s0378-5955(97)00046-4 [PubMed: 9213127]

Shepherd RK, & Javel E (1999). Electrical stimulation of the auditory nerve: II. Effect of stimulus waveshape on single fibre response properties. Hearing Research, 130(1-2), 171–188. 10.1016/s0378-5955(99)00011-8 [PubMed: 10320107]

Shepherd RK, Linahan N, Xu J, Clark GM, & Arak S (1999). Chronic electrical stimulation of the auditory nerve using non-charge-balanced stimuli. Acta Oto-Laryngologica, 119(6), 674–684. 10.1080/00016489950180621 [PubMed: 10587001]

Shepherd RK, Matsushima J, Millard RE, & Clark GM (1991). Cochlear pathology following chronic electrical stimulation using non charge balanced stimuli. Acta Oto-Laryngologica, 111(5), 848–860. 10.3109/00016489109138421 [PubMed: 1759570]

Shepherd RK, Roberts LA, & Paolini AG (2004). Long-term sensorineural hearing loss induces functional changes in the rat auditory nerve. European Journal of Neuroscience, 20(11), 3131–3140. 10.1111/j.1460-9568.2004.03809.x [PubMed: 15579167]

Skidmore J, Carter BL, Riggs WJ, & He S (2022a). The effect of advanced age on the electrode-neuron interface in cochlear implant users. Ear and Hearing, 43(4), 1300–1315. 10.1097/aud.0000000000001185 [PubMed: 34935648]

Skidmore J, & He S (2021). The effect of increasing interphase gap on N1 latency of the electrically evoked compound action potential and the stimulation level offset in human cochlear implant users. Ear and Hearing, 42(1), 180–192. 10.1097/aud.0000000000000919 [PubMed: 32826505]

Skidmore J, Ramekers D, Colesa DJ, Schvartz-Leyzac KC, Pfingst BE, & He S (2022b). A broadly applicable method for characterizing the slope of the electrically evoked compound action potential amplitude growth function. Ear and Hearing, 43(1), 150–164. 10.1097/aud.0000000000001084 [PubMed: 34241983]

Skidmore J, Xu L, Chao X, Riggs WJ, Pellittieri A, Vaughan C, Ning X, Wang R, Luo J, & He S (2021). Prediction of the functional status of the cochlear nerve in individual cochlear implant users using machine learning and electrophysiological measures. Ear and Hearing, 42(1), 180–192. 10.1097/aud.0000000000000916 [PubMed: 32826505]

Smit JE, Hanekom T, & Hanekom JJ (2008). Predicting action potential characteristics of human auditory nervefibres through modification of the Hodgkin-Huxley equations. South AfricanJournal of Science, 104(7), 284–292.

Smit JE, Hanekom T, & Hanekom JJ (2009). Modelled temperature-dependent excitability behaviour of a single ranvier node for a human peripheral sensory nerve fibre. Biological Cybernetics, 100(1), 49–58. 10.1007/s00422-008-0280-7 [PubMed: 19066936]

Smit JE, Hanekom T, van Wieringen A, Wouters J, & Hanekom JJ (2010). Threshold predictions of different pulse shapes using a human auditory nerve fibre model containing persistent sodium and slow potassium currents. Hearing Research, 269(1-2), 12–22. 10.1016/j.heares.2010.08.004 [PubMed: 20708672]

Spoendlin H, & Schrott A (1989). Analysis of the human auditory nerve. Hearing Research, 43(1), 25–38. 10.1016/0378-5955(89)90056-7 [PubMed: 2613564]

Spitzer ER, & Hughes ML (2017). Effect of stimulus polarity on physiological spread of excitation in cochlear implants. Journal of the American Academy of Audiology, 28(09), 786–798. 10.3766/jaaa.16144 [PubMed: 28972468]

Stypulkowski PH, & van den Honert C (1984). Physiological properties of the electrically stimulated auditory nerve. I. Compound action potential recordings. Hearing Research, 14(3), 205–223. 10.1016/0378-5955(84)90051-0 [PubMed: 6480510]

Tabibi S, Kegel A, Lai WK, Bruce IC, & Dillier N (2019). Measuring temporal response properties of auditory nerve fibers in cochlear implant recipients. Hearing Research, 380, 187–196. 10.1016/j.heares.2019.07.004 [PubMed: 31325737]

Takanen M, Strahl S, Schwarz K (2022). Predicting objective measures of the electrode-neuron interface with an auditory model. 19th International Symposium on Hearing: Psychoacoustics, Physiology of Hearing, and Auditory Modelling, from the Ear to the Brain (ISH2022), Lyon, France. Zenodo. 10.5281/zenodo.6576891

Tejani VD, Abbas PJ, & Brown CJ (2017). Relationship between peripheral and psychophysical measures of amplitude modulation detection in cochlear implant users. Ear and Hearing, 38(5), e268–e284. 10.1097/aud.0000000000000417 [PubMed: 28207576]

Trinh T-T, Cohen C, Boullaud L, Cottier JP, & Bakhos D (2021). Sheep as a large animal model for cochlear implantation. Brazilian Journal of Otorhinolaryngology. 10.1016/j.bjorl.2021.02.014

Undurraga JA, Carlyon RP, Wouters J, & van Wieringen A (2013). The polarity sensitivity of the electrically stimulated human auditory nerve measured at the level of the brainstem. Journal of the Association for Research in Otolaryngology, 14(3), 359–377. 10.1007/s10162-013-0377-0 [PubMed: 23479187]

Undurraga JA, van Wieringen A, Carlyon RP, Macherey O, & Wouters J (2010). Polarity effects on neural responses of the electrically stimulated auditory nerve at different cochlear sites. Hearing Research, 269(1-2), 146–161. 10.1016/j.heares.2010.06.017 [PubMed: 20600739]

van den Honert C, & Mortimer JT (1979). The response of the myelinated nerve fiber to short duration biphasic stimulating currents. Annals of Biomedical Engineering, 7(2), 117–125. 10.1007/bf02363130 [PubMed: 533020]

van den Honert C, & Stypulkowski PH (1984). Physiological properties of the electrically stimulated auditory nerve. II. Single fiber recordings. Hearing Research, 14(3), 225–243. 10.1016/0378-5955(84)90052-2 [PubMed: 6480511]

van den Honert C, & Stypulkowski PH (1987). Temporal response patterns of single auditory nerve fibers elicited by periodic electrical stimuli. Hearing Research, 29(2-3), 207–222. 10.1016/0378-5955(87)90168-7 [PubMed: 3624084]

van Gendt MJ, Briaire JJ, & Frijns JHM (2019). Effect of neural adaptation and degeneration on pulse-train ECAPs: A model study. Hearing Research, 377, 167–178. 10.1016/j.heares.2019.03.013 [PubMed: 30947041]

van Gendt MJ, Siebrecht M, Briaire JJ, Bohte SM, & Frijns JHM (2020). Short and long-term adaptation in the auditory nerve stimulated with high-rate electrical pulse trains are better described by a power law. Hearing Research, 398, 108090. 10.1016/j.heares.2020.108090 [PubMed: 33070033]

van Wieringen A, Carlyon RP, Laneau J, & Wouters J (2005). Effects of waveform shape on human sensitivity to electrical stimulation of the inner ear. Hearing Research, 200(1-2), 73–86. 10.1016/j.heares.2004.08.006 [PubMed: 15668040]

van Wieringen A, Macherey O, Carlyon RP, Deeks JM, & Wouters J (2008). Alternative pulse shapes in electrical hearing. Hearing Research, 242(1-2), 154–163. 10.1016/j.heares.2008.03.005 [PubMed: 18468821]

Viana LM, O'Malley JT, Burgess BJ, Jones DD, Oliveira CACP, Santos F, Merchant SN, Liberman LD, & Liberman MC (2015). Cochlear neuropathy in human presbycusis: Confocal analysis of hidden hearing loss in post-mortem tissue. Hearing Research, 327, 78–88. 10.1016/j.heares.2015.04.014 [PubMed: 26002688]

Vink HA, van Dorp WC, Thomeer HGXM, Versnel H, & Ramekers D (2020). BDNF outperforms TrkB agonist 7,8,3′-THF in preserving the auditory nerve in deafened Guinea pigs. Brain Sciences, 10(11), 787. 10.3390/brainsci10110787 [PubMed: 33126525]

Wark B, Lundstrom BN, & Fairhall A (2007). Sensory adaptation. Current Opinion in Neurobiology, 17(4), 423–429. 10.1016/j.conb.2007.07.001 [PubMed: 17714934]

Wiemes GRM, Hamerschmidt R, Moreira ATR, de Fraga R, Tenório SB, & Carvalho B (2016). Auditory nerve recovery function in cochlear implant surgery with local anesthesia and sedation versus general anesthesia. Audiology and Neurotology, 21(3), 150–157. 10.1159/000445098 [PubMed: 27161843]

Wilson BS, Finley CC, Lawson DT, Wolford RD, Eddington DK, & Rabinowitz WM (1991). Better speech recognition with cochlear implants. Nature, 352(6332), 236–238. 10.1038/352236a0 [PubMed: 1857418]

Wilson BS, Finley CC, Lawson DT, & Zerbi M (1997). Temporal representations with cochlear implants. The American Journal of Otology, 18(6), S30–34. [PubMed: 9391587]

Woo J, Miller CA, & Abbas PJ (2009a). Biophysical model of an auditory nerve fiber with a novel adaptation component. IEEE Transactions on Biomedical Engineering, 56(9), 2177–2180. 10.1109/tbme.2009.2023978 [PubMed: 19497810]

Woo J, Miller CA, & Abbas PJ (2009b). Simulation of the electrically stimulated cochlear neuron: Modeling adaptation to trains of electric pulses. IEEE Transactions on Biomedical Engineering, 56(5), 1348–1359. 10.1109/tbme.2008.2005782 [PubMed: 19473930]

Woo J, Miller CA, & Abbas PJ (2010). The dependence of auditory nerve rate adaptation on electric stimulus parameters, electrode position, and fiber diameter: A computer model study. Journal of the Association for Research in Otolaryngology, 11(2), 283–296. 10.1007/s10162-009-0199-2 [PubMed: 20033248]

Wu PZ, Liberman LD, Bennett K, de Gruttola V, O'Malley JT, & Liberman MC (2019). Primary neural degeneration in the human cochlea: Evidence for hidden hearing loss in the aging ear. Neuroscience, 407, 8–20. 10.1016/j.neuroscience.2018.07.053 [PubMed: 30099118]

Xu L, Skidmore J, Luo J, Chao X, Wang R, Wang H, & He S (2020). The effect of pulse polarity on neural response of the electrically stimulated cochlear nerve in children with cochlear nerve deficiency and children with normal-sized cochlear nerves. Ear and Hearing, 41(5), 1306–1319. 10.1097/aud.0000000000000854 [PubMed: 32141933]

Yuan Y, Skidmore J, & He S (2022). Interpreting the interphase gap effect on the electrically evoked compound action potential. JASA Express Letters, 2(2), 027201. 10.1121/10.0009383 [PubMed: 35156092]

Zhang F, Benson C, Murphy D, Boian M, Scott M, Keith R, Xiang J, & Abbas P (2013). Neural adaptation and behavioral measures of temporal processing and speech perception in cochlear implant recipients. PLoS One, 8(12), e84631. 10.1371/journal.pone.0084631 [PubMed: 24386403]

Zhang F, Miller CA, Robinson BK, Abbas PJ, & Hu N (2007). Changes across time in spike rate and spike amplitude of auditory nerve fibers stimulated by electric pulse trains. Journal of the Association for Research in Otolaryngology, 8(3), 356–372. 10.1007/s10162-007-0086-7 [PubMed: 17562109]

Zhou R, Abbas PJ, & Assouline JG (1995). Electrically evoked auditory brainstem response in peripherally myelin-deficient mice. Hearing Research, 88(1-2), 98–106. 10.1016/0378-5955(95)00105-d [PubMed: 8576009]

Zilany MSA, Bruce IC, Nelson PC, & Carney LH (2009). A phenomenological model of the synapse between the inner hair cell and auditory nerve: Long-term adaptation with power-law dynamics.

The Journal of the Acoustical Society of America, 126(5), 2390–2412. 10.1121/1.3238250 [PubMed: 19894822]

Zimmermann CE, Burgess BJ, & Nadol JB (1995). Patterns of degeneration in the human cochlear nerve. Hearing Research, 90(1-2), 192–201. 10.1016/0378-5955(95)00165-1 [PubMed: 8974997]

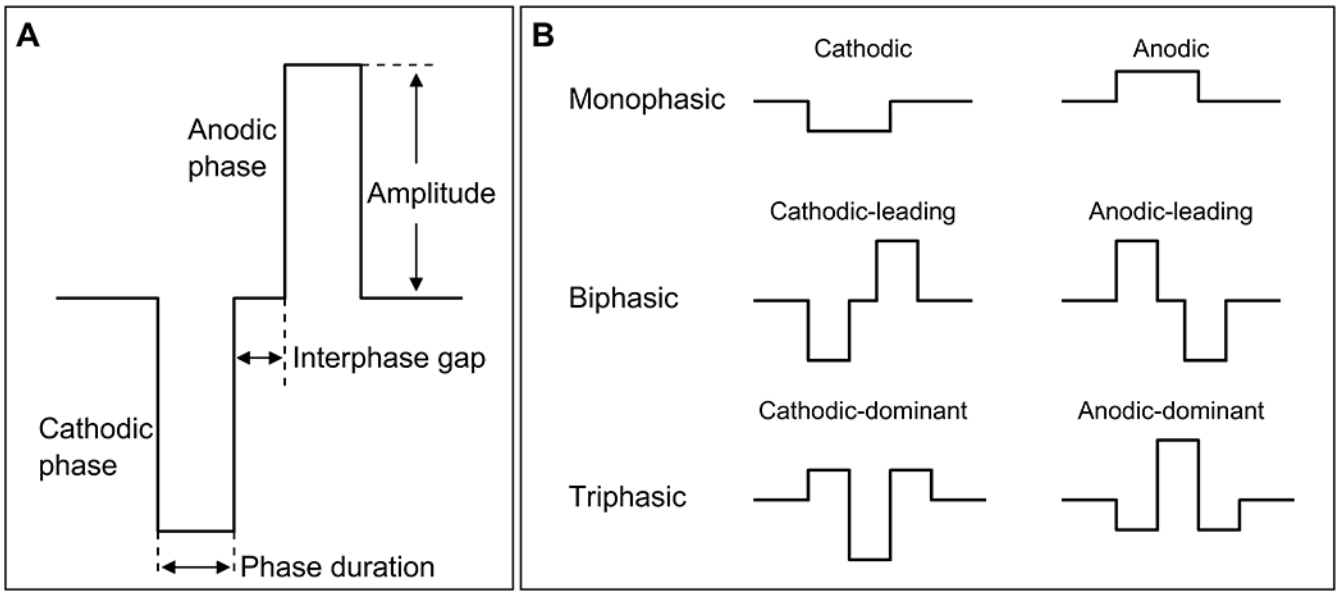

Figure 1.

Illustrations of various pulse shapes for single pulse stimulation. A) Example biphasic single pulse with the pulse amplitude, polarity, phase duration, and interphase gap indicated. B) Example monophasic, biphasic, and triphasic single pulses with for cathodic (left column) and anodic (right column) stimulation.

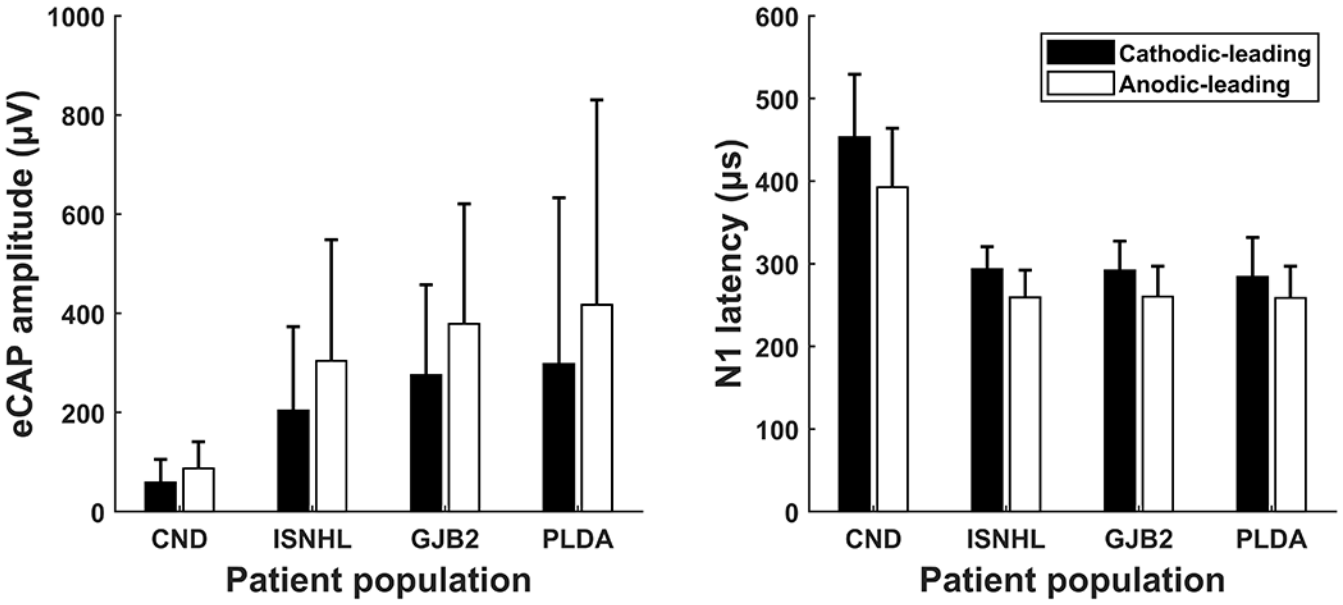

Figure 2.

The means and standard deviations of electrically evoked compound action potential (eCAP) amplitude (left panel) and N1 latency (right panel) measured with cathodic-leading (black bars) and anodic-leading (white bars) biphasic single pulse stimuli for 30 children (91 electrodes tested) with cochlear nerve deficiency (CND), 32 children (98 electrodes tested) with idiopathic sensorineural hearing loss (ISNHL), 19 children (54 electrodes tested) with Gap Junction Beta-2 genetic mutation (GJB2), 15 and post-lingually deafened adults (PLDA, 50 electrodes tested).

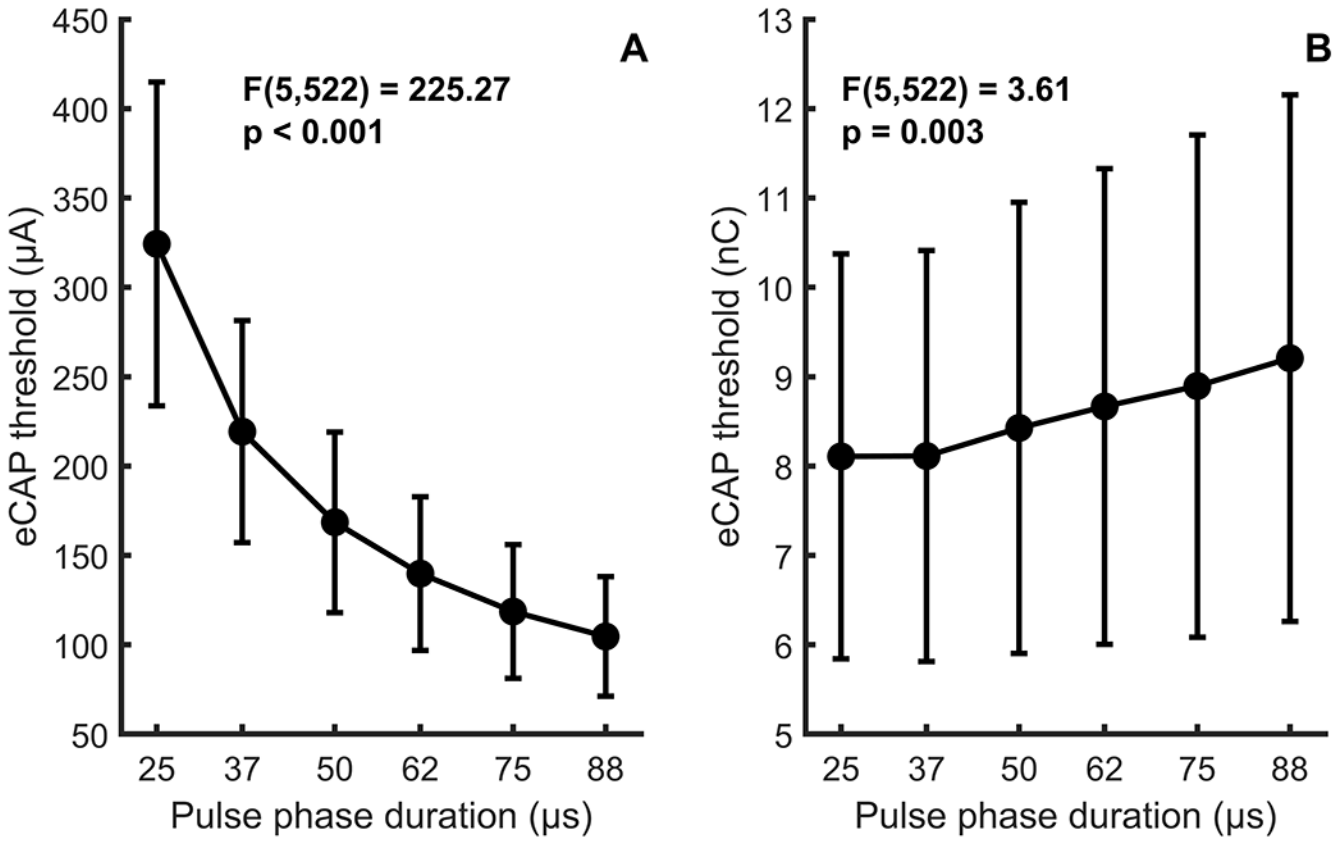

Figure 3.

The means and standard deviations of electrically evoked compound action potential (eCAP) thresholds measured for six pulse phase durations in pediatric cochlear implant users (88 electrodes across 30 ears). The eCAP thresholds are presented in units of microamps (μA, Panel A) and nanocoulombs (nC, Panel B). The results from linear mixed-effects models are also provided in each panel.

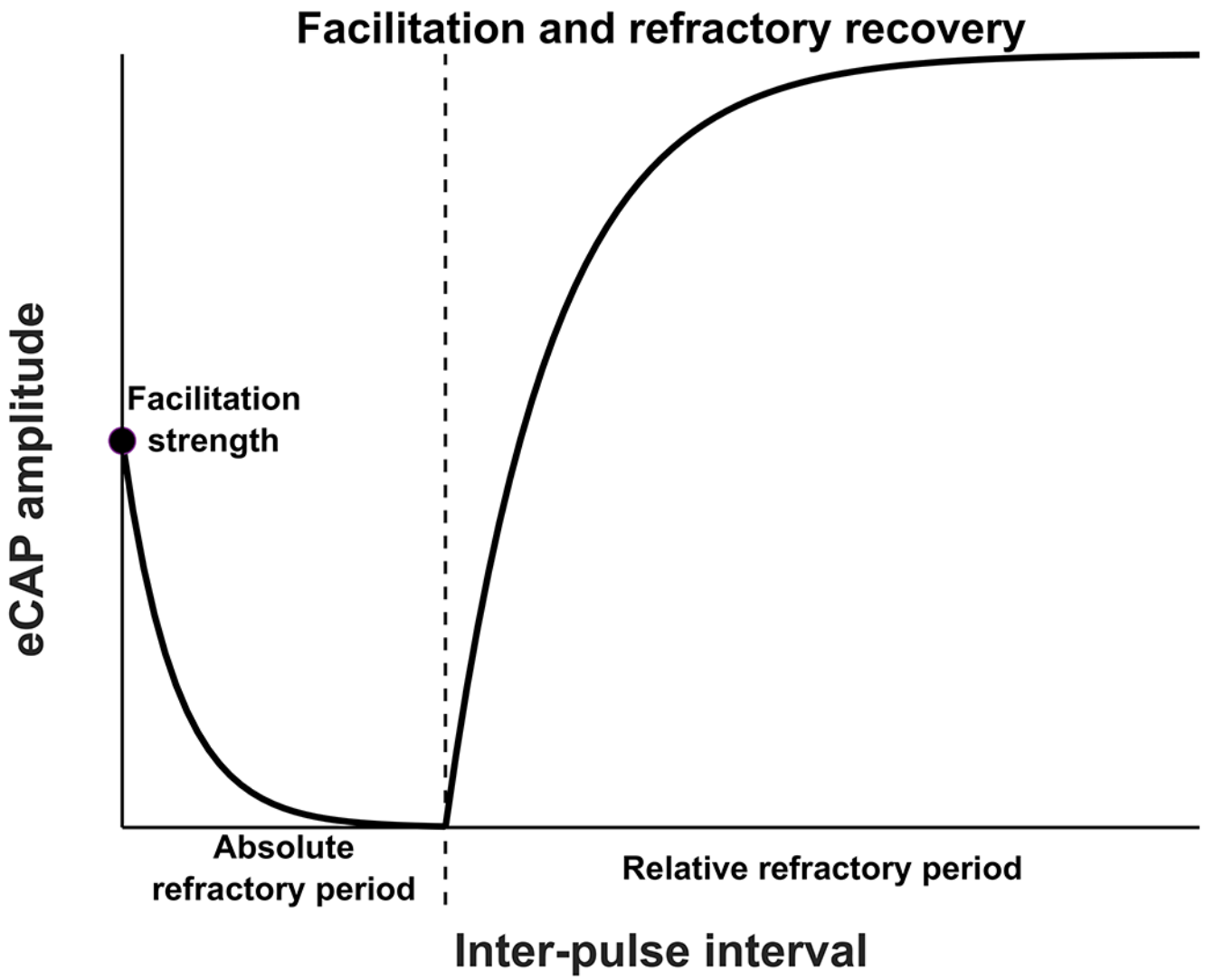

Figure 4.
A schematic illustration of facilitation and refractory recovery functions, and parameters that can be estimated by the functions.

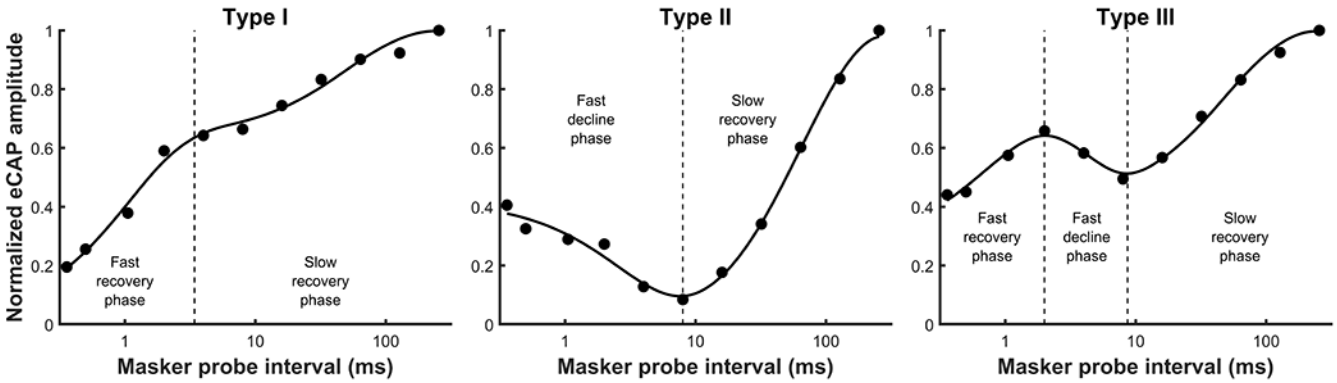

Figure 5.

Illustrations of each type of neural adaptation recovery function, along with indications of the phases of each function.

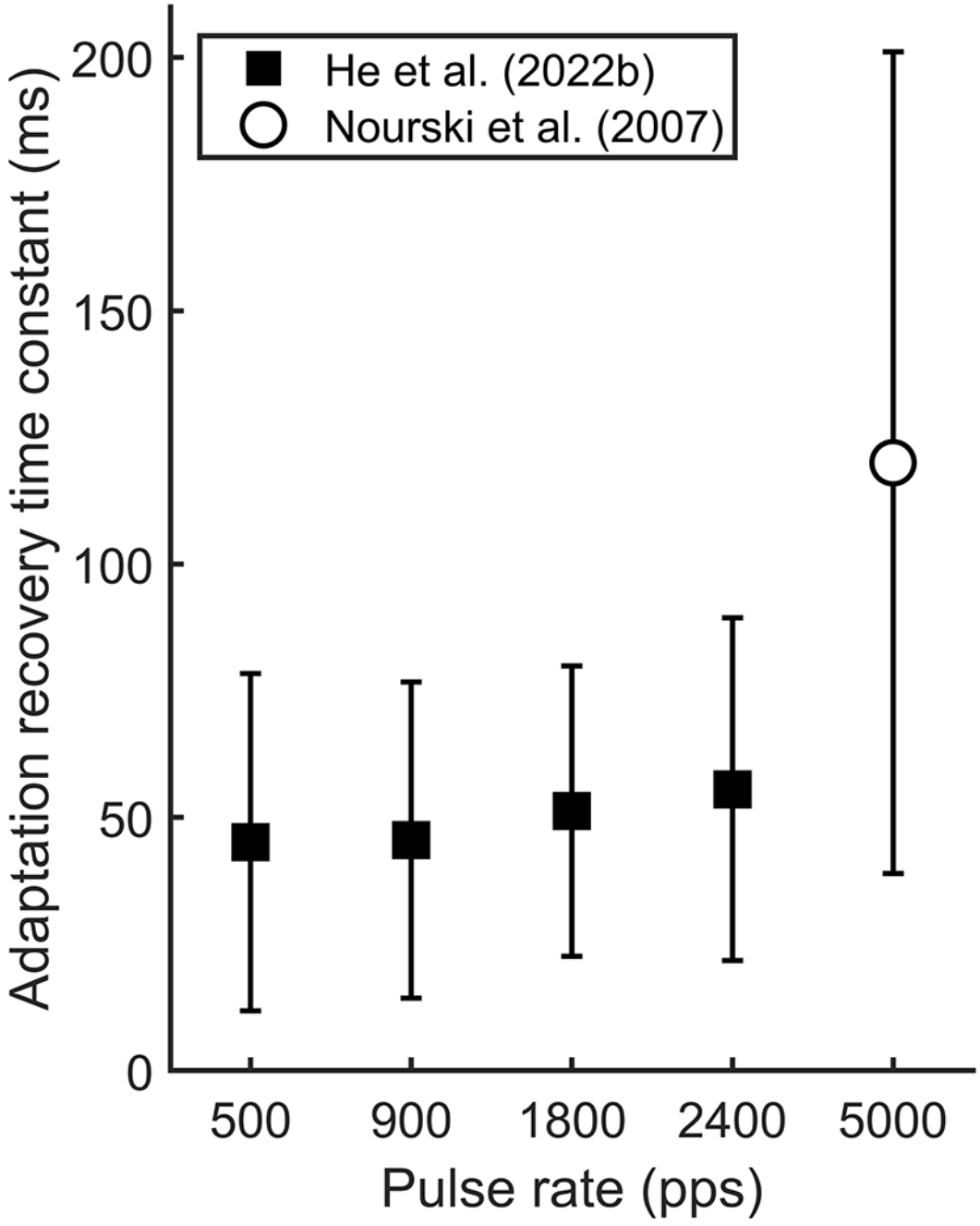

Figure 6.

The means and standard deviations of adaptation recovery time constants measured in human cochlear implant users (He et al., 2022b) and in guinea pigs (Nourski et al., 2007). The time constants were estimated using similar mathematical models.

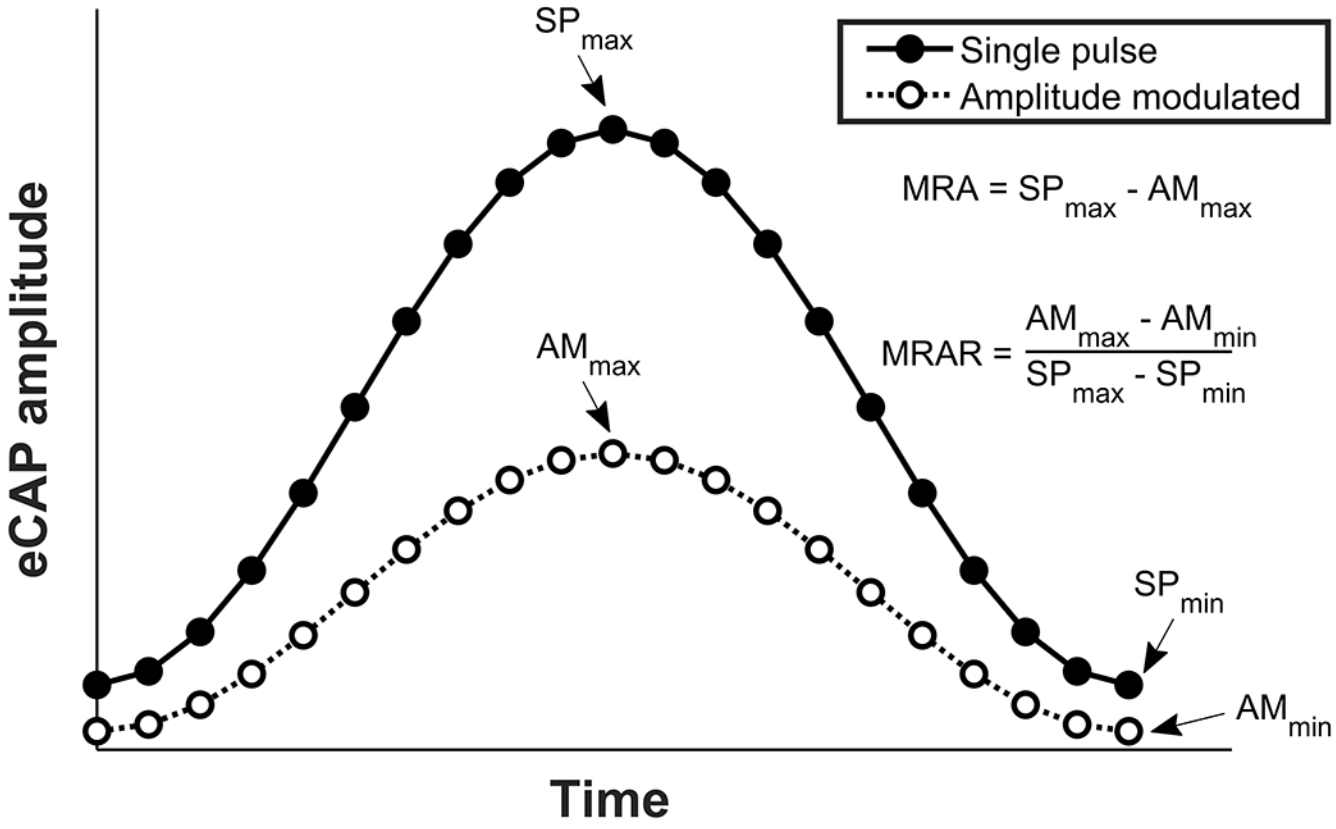

Figure 7.
An illustration demonstrating the calculation of the modulated response amplitude (MRA) and the modulated response amplitude ratio (MRAR).

TABLE 1.

The means (standard deviations) of neural adaptation time constants (β_1 – fast phase, β_2 – slow phase) estimated using a power law function at four pulse rates. pps, pulses per second.

Pulse rate (pps)	β_1	β_2
500	−28.14 (20.98)	-0.049 (0.039)
900	−47.06 (28.19)	−0.097 (0.055)
1800	−72.55 (−23.45)	−0.132 (0.090)
2400	−79.15 (18.28)	−0.178 (0.108)